Kittel Chapter 9 Fermi Surfaces and Metals

Part 1

Few people would define a *metal* as " *a solid with a Fermi surface*."

This may nevertheless be the most meaningful definition of a metal one can give today; It represents a profound advance in the understanding of why metals behave as they do. The concept of the *Fermi surface*, as developed by quantum physics, provides a precise explanation of the main physical properties of metals.

A. R. Mackintosh

(1936-1995)

Magnetism and neutron scattering; rare-earth metals; solid-state physics

Kittel Chapter 6

FREE ELECTRON GAS IN THREE DIMENSIONS

$$-\frac{\hbar^2}{2m} \left(\frac{\partial^2}{\partial x^2} + \frac{\partial^2}{\partial y^2} + \frac{\partial^2}{\partial z^2} \right) \psi_{\mathbf{k}}(\mathbf{r}) = \epsilon_{\mathbf{k}} \psi_{\mathbf{k}}(\mathbf{r}) . \tag{6}$$

Periodic boundary conditions

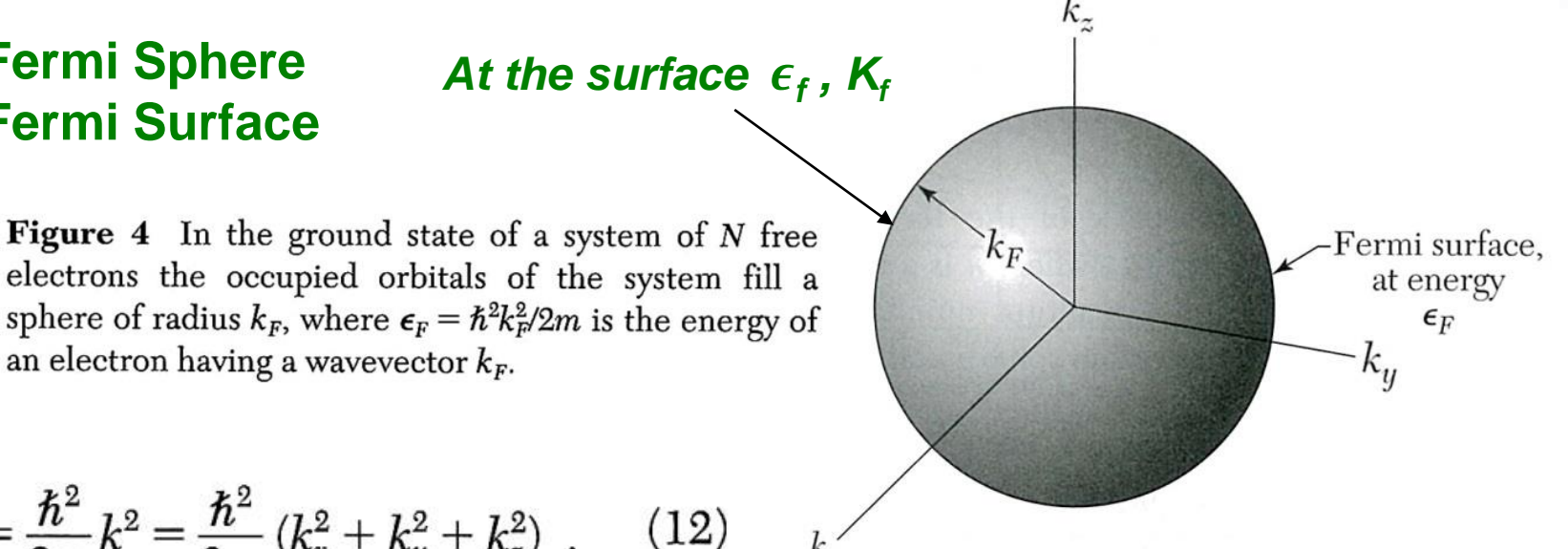
$$\psi(x+L,y,z)=\psi(x,y,z) , \qquad (8)$$

Wave functions satisfying the free particle Schrödinger equation, and the periodicity condition are of the form of a traveling plane wave:

$$\psi_{\mathbf{k}}(\mathbf{r}) = \exp(i\mathbf{k} \cdot \mathbf{r}) , \qquad \qquad Exp(ikL) = 1$$

$$k = \pm n \ 2\pi / L \qquad (9)$$

Fermi Sphere Fermi Surface



electrons the occupied orbitals of the system fill a sphere of radius
$$k_F$$
, where $\epsilon_F = \hbar^2 k_F^2 / 2m$ is the energy of an electron having a wavevector k_F .

$$\epsilon_{\mathbf{k}} = \frac{\hbar^2}{2m} k^2 = \frac{\hbar^2}{2m} (k_x^2 + k_y^2 + k_z^2) .$$
 (12)

the operator $\mathbf{p} = -i\hbar\nabla$,

$$\underline{\mathbf{p}\psi_{\mathbf{k}}}(\mathbf{r}) = -i\hbar\nabla\psi_{\mathbf{k}}(\mathbf{r}) = \underline{\hbar\mathbf{k}}\psi_{\mathbf{k}}(\mathbf{r}) , \qquad (13)$$

so that the plane wave ψ_k is an eigenfunction of the linear momentum with the eigenvalue $\hbar \mathbf{k}$.

In the ground state of a system of N free electrons, the occupied orbitals may be represented as points inside a sphere in \mathbf{k} space.

$$\epsilon_F = \frac{\hbar^2}{2m} k_F^2$$
 at the Fermi surface ϵ_F , k_f (14)

Free Electron Model

Nearly Free Electron Model

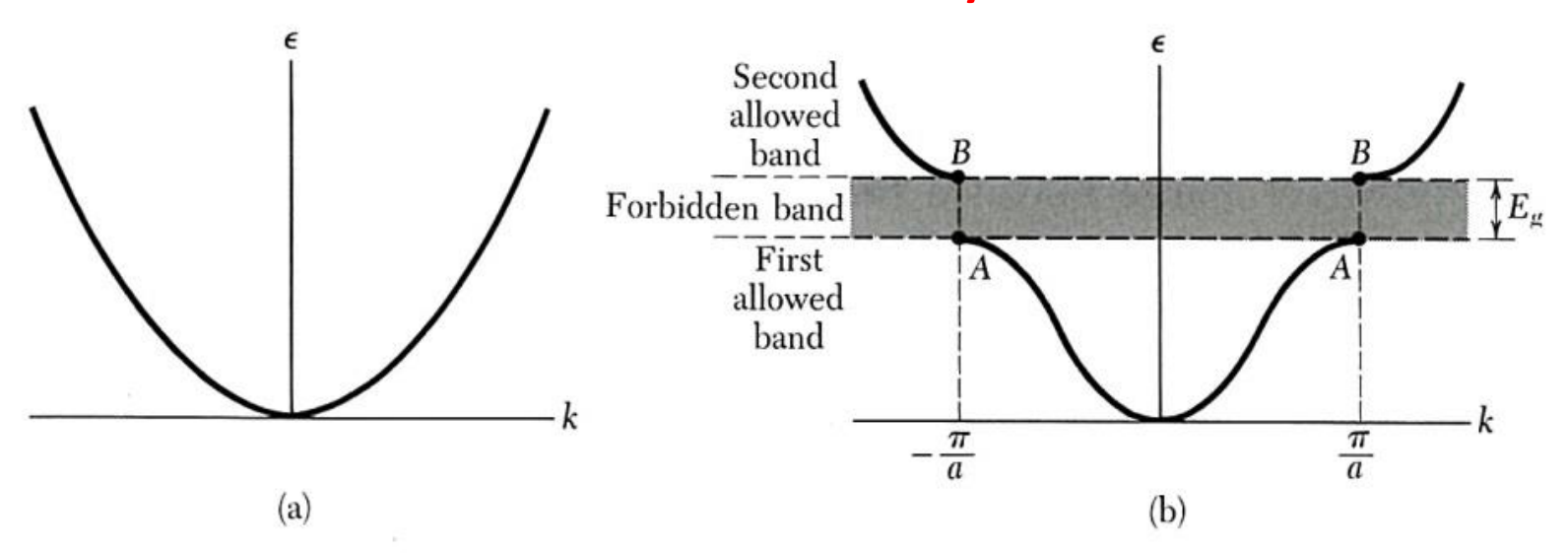


Figure 2 (a) Plot of energy ϵ versus wavevector k for a free electron. (b) Plot of energy versus wavevector for an electron in a monatomic linear lattice of lattice constant a. The energy gap E_g shown is associated with the first Bragg reflection at $k = \pm \pi/a$; other gaps are found at $\pm n\pi/a$, for integral values of n.

The Bragg condition $(k + G)^2 = k^2$ for diffraction of a wave of wavevector **k** becomes in one dimension

$$k = \pm \frac{1}{2}G = \pm n\pi/a,$$
 Solutions in 1-D (4)

Where $G = 2\pi n/a$ is a reciprocal lattice vector and \mathbf{n} is an integer. The first reflections and the first energy gap occur at $k = \pm \pi/a$. The region in \mathbf{k} space between - π/a and π/a is the **first Brillouin zone** of this lattice. Other energy gaps occur for other values of the integer \mathbf{n} .

The wavefunctions at $k = \pm \pi/a$ are not the traveling waves $\exp(i\pi x/a)$ or $\exp(-i\pi x/a)$ of free electrons. At these special values of k the wavefunctions are made up of equal parts of waves traveling to the right and to the left. When the Bragg reflection condition $k = \pm \pi/a$ is satisfied by the wavevector, a wave traveling to the right is Bragg-reflected to travel to the left, and vice versa. Each subsequent Bragg reflection will reverse the direction of travel of the wave. A wave that travels neither to the right nor to the left is a standing wave: it doesn't go anywhere.

The time-independent state is represented by standing waves. We can form two different standing waves from the two traveling waves $\exp(\pm i\pi x/a)$, namely

Standing wave solutions

$$\psi(+) = \exp(i\pi x/a) + \exp(-i\pi x/a) = 2\cos(\pi x/a) ;$$

$$\psi(-) = \exp(i\pi x/a) - \exp(-i\pi x/a) = 2i\sin(\pi x/a) .$$
(5)

The standing waves are labeled (+) or (-) according to whether or not they change sign when -x is substituted for x. Both standing waves are composed of equal parts of right- and left-directed traveling waves.

Origin of the Energy Gap

The two standing waves $\psi(+)$ and $\psi(-)$ pile up electrons at different regions, and therefore the two waves have different values of the potential energy. This is the origin of the energy gap. The probability density ρ of a particle is $\psi^*\psi = |\psi|^2$. For a pure traveling wave $\exp(ikx)$, we have $\rho = \exp(-ikx) \exp(ikx) = 1$, so that the charge density is constant. The charge density is not constant for linear combinations of plane waves. Consider the standing wave $\psi(+)$ in (5); for this we have

$$\rho(+) = |\psi(+)|^2 \propto \cos^2 \pi x/a .$$

This function piles up electrons (negative charge) on the positive ions centered at x = 0, a, 2a, . . . in Fig. 3, where the potential energy is lowest.

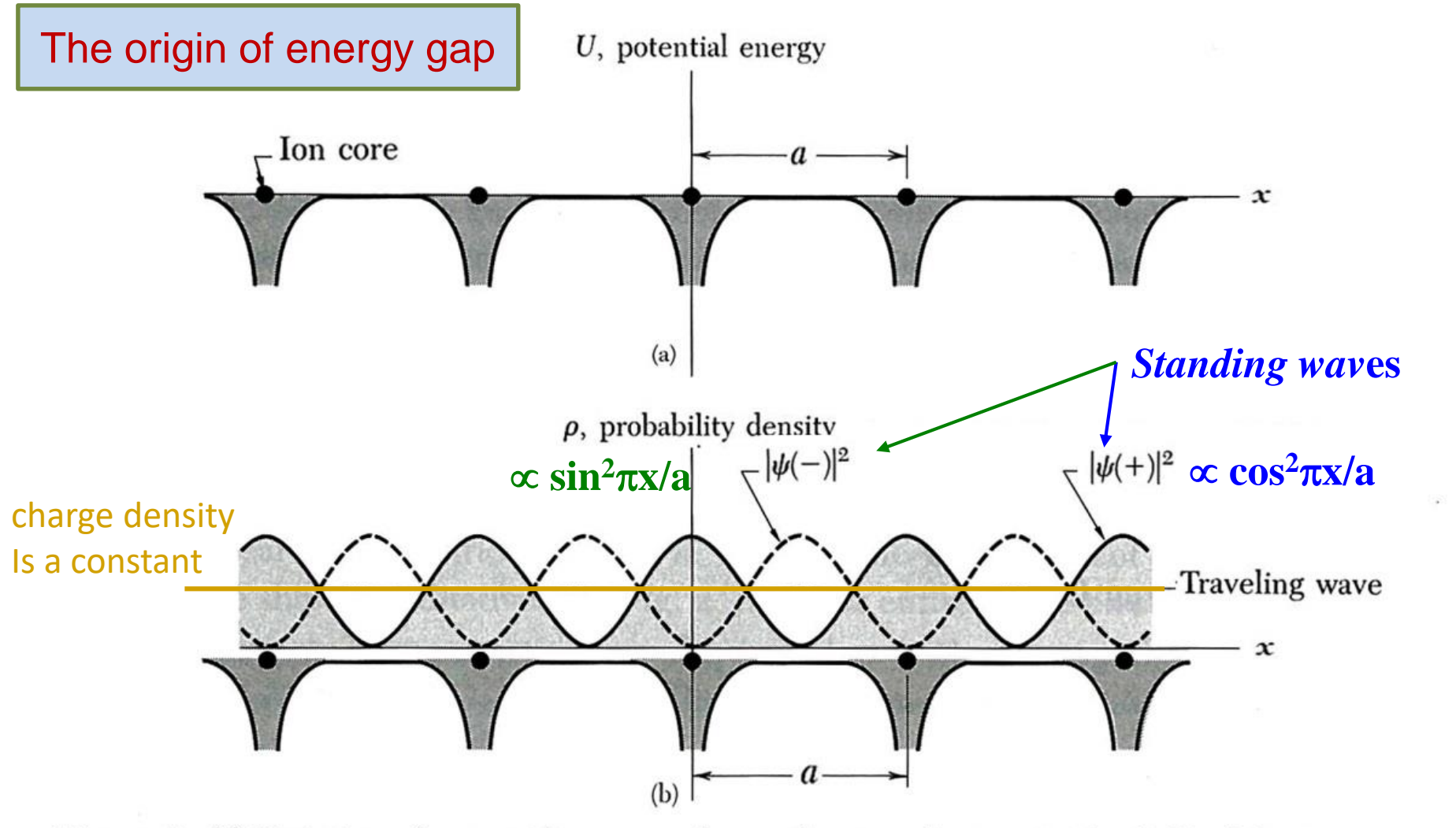


Figure 3 (a) Variation of potential energy of a conduction electron in the field of the ion cores of a linear lattice. (b) Distribution of probability density ρ in the lattice for $|\psi(-)|^2 \propto \sin^2 \pi x/a$; $|\psi(+)|^2 \propto \cos^2 \pi x/a$; and for a traveling wave. The wavefunction $\psi(+)$ piles up electronic charge on the cores of the positive ions, thereby lowering the potential energy in comparison with the average potential energy seen by a traveling wave. The wavefunction $\psi(-)$ piles up charge in the region between the ions, thereby raising the potential energy in comparison with that seen by a traveling wave. This figure is the key to understanding the origin of the energy gap.

Awarded the 1952 <u>Nobel Prize</u> for "their development of new ways and methods for nuclear magnetic precision measurements

Felix Bloch (1905-1983, Swiss)



BLOCH FUNCTIONS

F. Bloch proved the important theorem that the solutions of the Schrödinger equation for a periodic potential must be of a special form:

$$\psi_{\mathbf{k}}(\mathbf{r}) = u_{\mathbf{k}}(\mathbf{r}) \exp(i\mathbf{k} \cdot \mathbf{r}) ,$$
 (7)

where $u_{\mathbf{k}}(\mathbf{r})$ has the period of the crystal lattice with $\underline{u_{\mathbf{k}}(\mathbf{r}) = u_{\mathbf{k}}(\mathbf{r} + \mathbf{T})}$. The result (7) expresses the Bloch theorem:

The eigenfunctions of the wave equation for a periodic potential are the product of a plane wave $\exp(i\mathbf{k}\cdot\mathbf{r})$ times a function $u_{\mathbf{k}}(\mathbf{r})$ with the periodicity of the crystal lattice.

A one-electron wavefunction of the form (7) is called a Bloch function and can be decomposed into a sum of traveling waves, as we see later. Bloch functions can be assembled into localized wave packets to represent electrons that propagate freely through the potential field of the ion cores.

Restatement of the Bloch Theorem

Once we determine the C's from (27), the wavefunction (25) is given as

$$\psi_k(x) = \sum_G C(k - G) e^{i(k - G)x} , \qquad (29)$$

which may be rearranged as

$$\psi_k(x) = \left(\sum_G C(k-G) e^{-iGx}\right) e^{ikx} = e^{ikx} u_k(x) ,$$

with the definition

$$u_k(x) \equiv \sum_G C(k-G) e^{-iGx} .$$

Because $u_k(x)$ is a Fourier series over the reciprocal lattice vectors, it is invariant under a crystal lattice translation T, so that $\underline{u_k(x) = u_k(x+T)}$. We verify this directly by evaluating $u_k(x+T)$:

$$u_k(x+T) = \sum C(k-G) \ e^{-iG(x+T)} = e^{-iGT} [\sum C(k-G) \ e^{-iGx}] = e^{-iGT} \ u_k(x) \ .$$

Because $\exp(-iGT) = 1$ by (2.17), it follows that $u_k(x + T) = u_k(x)$, thereby establishing the periodicity of u_k . This is an alternate and exact proof of the Bloch theorem and is valid even when the ψ_k are degenerate.

Fermi surface

The Fermi surface is the surface of constant energy ϵ_F in k space. The Fermi surface separates the unfilled orbitals from the filled orbitals, at absolute zero. The electrical properties of the metal are determined by the shape of the Fermi surface, because the current is due to changes in the occupancy of states near the Fermi surface.

The shape may be very intricate in a reduced zone scheme and yet have a simple interpretation when reconstructed to lie near the surface of a sphere. We exhibit in Fig. 1 the free electron Fermi surfaces constructed for two metals that have the face-centered cubic crystal structure: copper, with one valence electron, and aluminum, with three. The free electron Fermi surfaces were developed from spheres of radius k_F determined by the valence electron concentration. How do we construct these surfaces from a sphere? The constructions require the reduced and periodic zone schemes.

The shape of Fermi surface of copper is deformed by interaction with the lattice.

fcc → reciprocal lattice → bcc

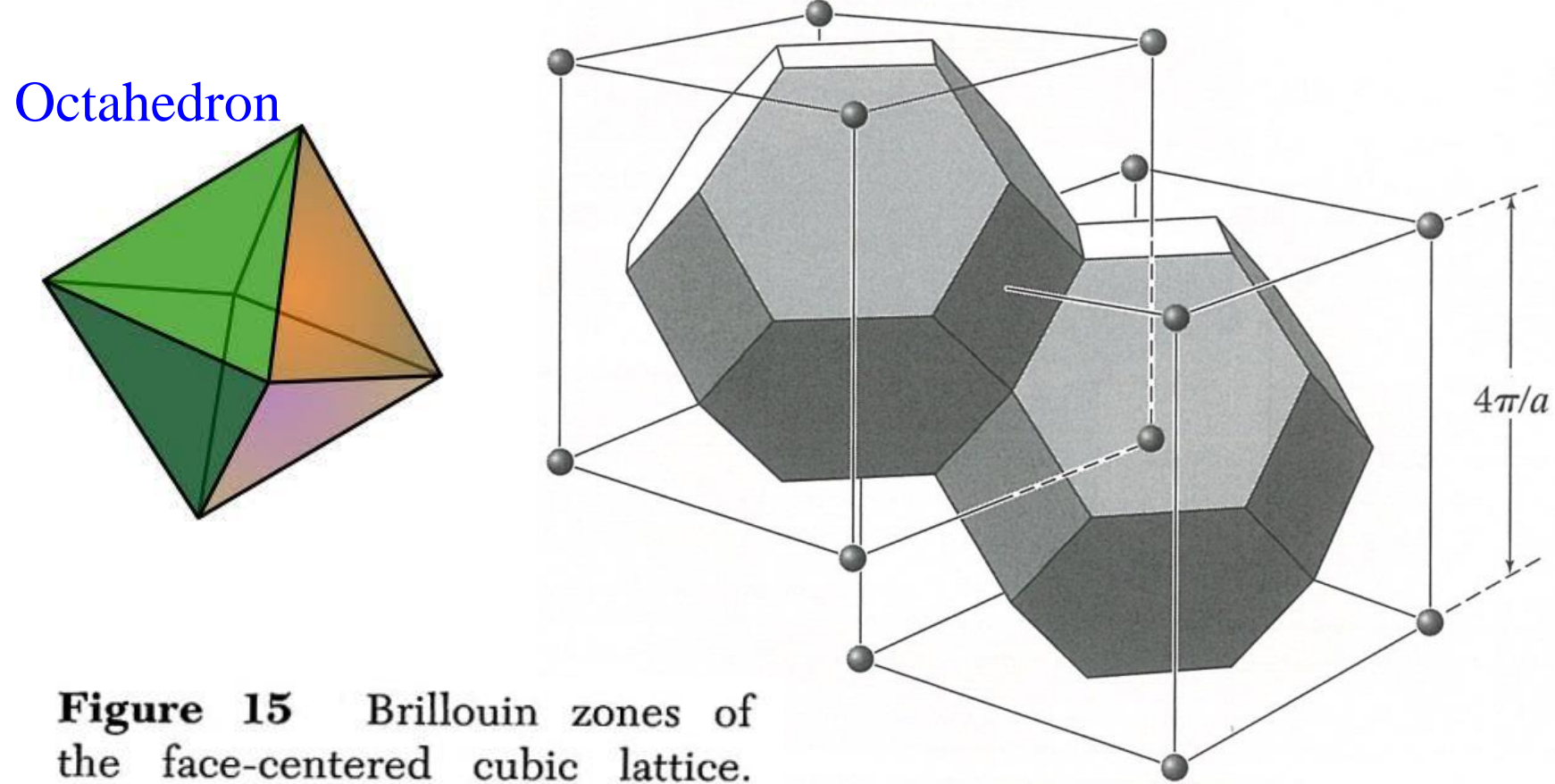
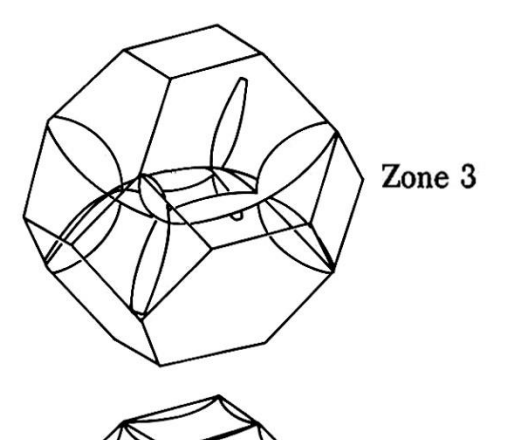


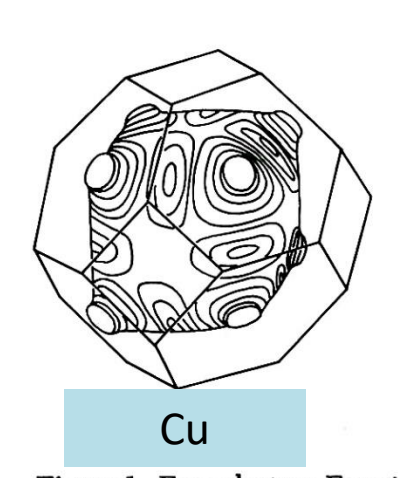
Figure 15 Brillouin zones of the face-centered cubic lattice. The cells are in reciprocal space, and the reciprocal lattice is body centered.

Brillouin zone in reciprocal space: Truncated Octahedron



Also refer to page 20, Fig. 8

The shape of Fermi surface of copper is deformed due to the interaction with the lattice.



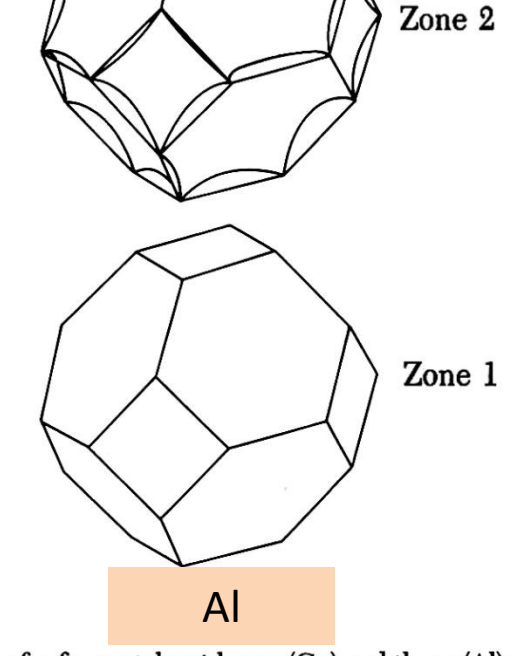


Figure 1 Free electron Fermi surfaces for fcc metals with one (Cu) and three (Al) valence electrons per primitive cell. The Fermi surface shown for copper has been deformed from a sphere to agree with the experimental results. The second zone of aluminum is nearly half-filled with electrons. (A. R. Mackintosh.)

Reduced Zone Scheme

It is always possible to select the wavevector index k of any Bloch function to lie within the first Brillouin zone. The procedure is known as mapping the band in the reduced zone scheme.

If we encounter a Bloch function written as $\psi_{\mathbf{k}'}(\mathbf{r}) = e^{i\mathbf{k}'\cdot\mathbf{r}}u_{\mathbf{k}'}(\mathbf{r})$, with \mathbf{k}' outside the first zone, as in Fig. 2, we may always find a suitable reciprocal lattice vector \mathbf{G} such that $\mathbf{k} = \mathbf{k}' + \mathbf{G}$ lies within the first Brillouin zone. Then

$$\psi_{\mathbf{k}'}(\mathbf{r}) = e^{i\mathbf{k}'\cdot\mathbf{r}}u_{\mathbf{k}'}(\mathbf{r}) = e^{i\mathbf{k}\cdot\mathbf{r}}(e^{-i\mathbf{G}\cdot\mathbf{r}}u_{\mathbf{k}'}(\mathbf{r}))$$

$$\equiv e^{i\mathbf{k}\cdot\mathbf{r}}u_{\mathbf{k}}(\mathbf{r}) = \psi_{\mathbf{k}}(\mathbf{r}) , \qquad (1)$$

where $u_{\mathbf{k}}(\mathbf{r}) \equiv e^{-i\mathbf{G}\cdot\mathbf{r}}u_{\mathbf{k}'}(\mathbf{r})$. Both $e^{-i\mathbf{G}\cdot\mathbf{r}}$ and $u_{\mathbf{k}'}(\mathbf{r})$ are periodic in the crystal lattice, so $u_{\mathbf{k}}(\mathbf{r})$ is also, whence $\psi_{\mathbf{k}}(\mathbf{r})$ is of the Bloch form.

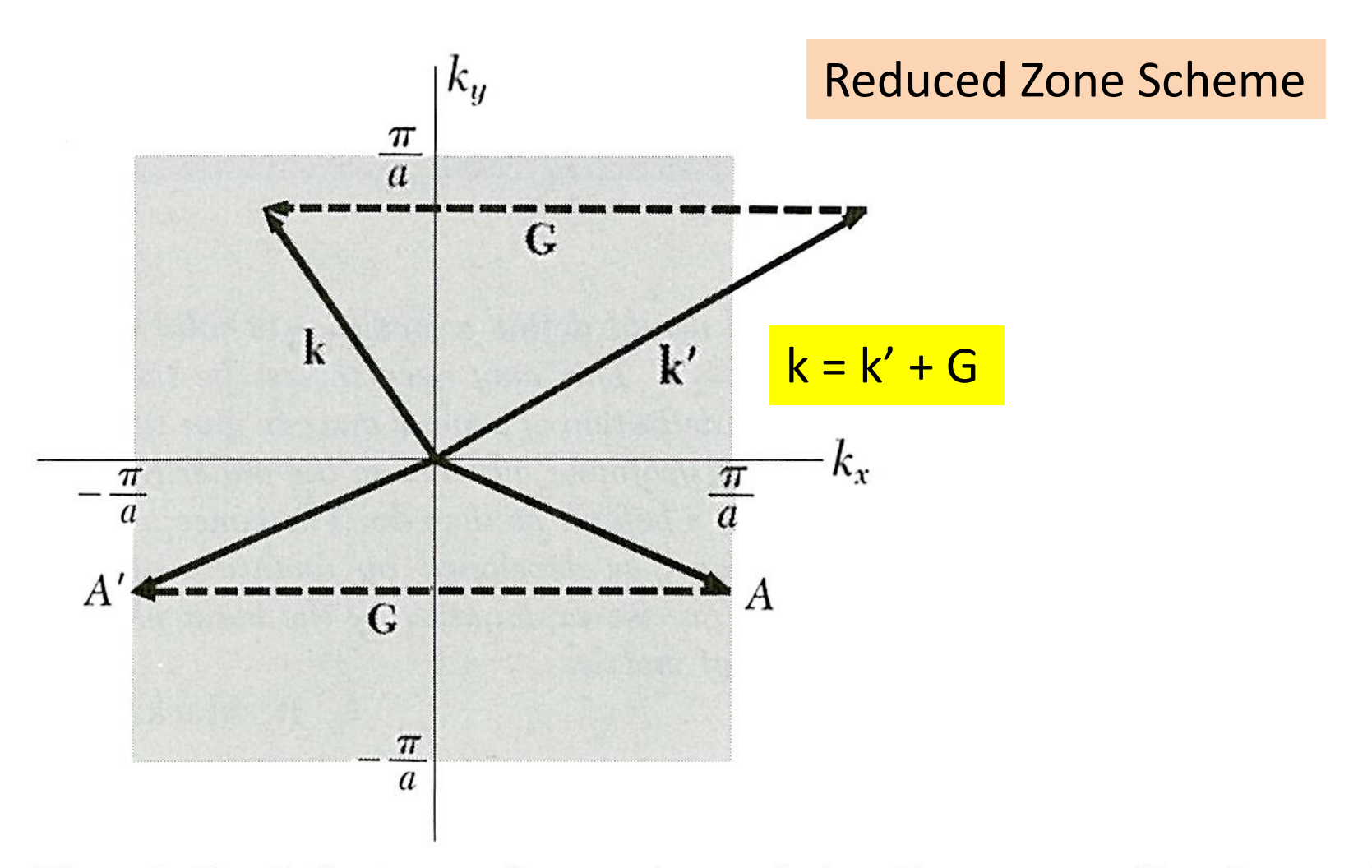


Figure 2 First Brillouin zone of a square lattice of side a. The wavevector \mathbf{k}' can be carried into the first zone by forming $\mathbf{k}' + \mathbf{G}$. The wavevector at a point A on the zone boundary is carried by \mathbf{G} to the point A' on the opposite boundary of the same zone. Shall we count both A and A' as lying in the first zone? Because they can be connected by a reciprocal lattice vector, we count them as *one* identical point in the zone.

Even with free electrons it is useful to work in the reduced zone scheme, as in Fig. 3. Any energy $\epsilon_{k'}$ for k' outside the first zone is equal to an ϵ_{k} in the first zone, where k = k' + G. Thus we need solve for the energy only in the first Brillouin zone, for each band. An energy band is a single branch of the ϵ_{k} versus k surface.

In the reduced zone scheme we should not be surprised to find different energies at the same value of the wavevector. Each different energy characterizes a different band.

Two wavefunctions at the same \mathbf{k} but of different energies will be independent of each other: the wavefunctions will be made up of different combinations of the plane wave components $\exp[i(\mathbf{k} + \mathbf{G}) \cdot \mathbf{r}]$ in the expansion of (7.29). Because the values of the coefficients $C(\mathbf{k} + \mathbf{G})$ will differ for the different bands we should add a symbol, say n, to the C's to serve as a band index: $C_n(\mathbf{k} + \mathbf{G})$. Thus the Bloch function for a state of wavevector \mathbf{k} in the band n can be written as

$$\psi_{n,\mathbf{k}} = \exp(i\mathbf{k} \cdot \mathbf{r})u_{n,\mathbf{k}}(\mathbf{r}) = \sum_{\mathbf{G}} C_n(\mathbf{k} + \mathbf{G}) \, \exp[i(\mathbf{k} + \mathbf{G}) \cdot \mathbf{r}] \ .$$

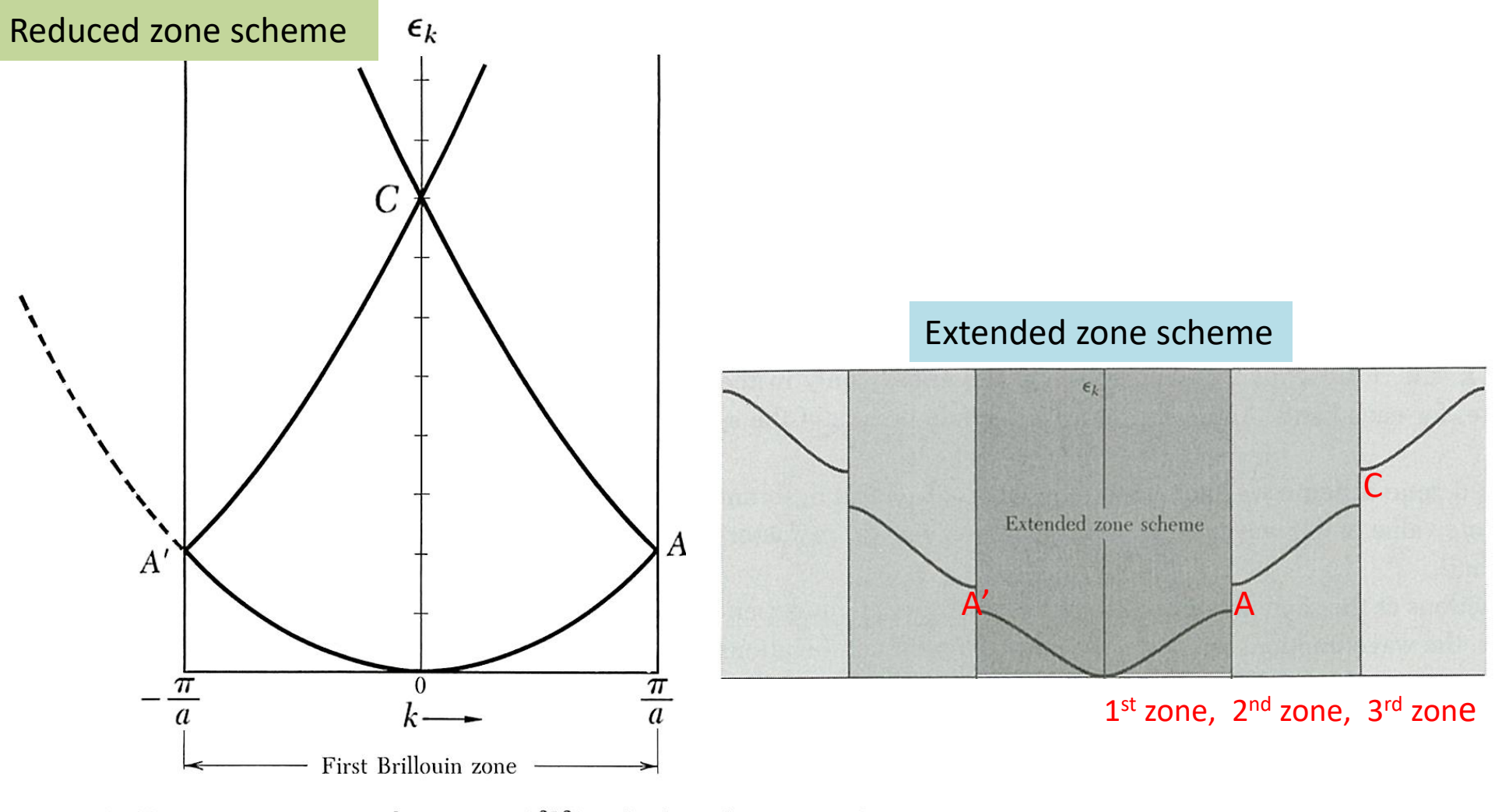


Figure 3 Energy-wavevector relation $\epsilon_k = \hbar^2 k^2 / 2m$ for free electrons as drawn in the reduced zone scheme. This construction often gives a useful idea of the overall appearance of the band structure of a crystal. The branch AC if displaced by $-2\pi/a$ gives the usual free electron curve for negative k, as suggested by the dashed curve. The branch A'C if displaced by $2\pi/a$ gives the usual curve for positive k. A crystal potential U(x) will introduce band gaps at the edges of the zone (as at A and A') and at the center of the zone (as at C). The point C when viewed in the extended zone scheme falls at the edges of the second zone. The overall width and gross features of the band structure are often indicated properly by such free electron bands in the reduced zone scheme.

Periodic Zone Scheme

We can repeat a given Brillouin zone periodically through all of wavevector space. To repeat a zone, we translate the zone by a reciprocal lattice vector. If we can translate a band from other zones into the first zone, we can translate a band in the first zone into every other zone. In this scheme the energy ϵ_k of a band is a periodic function in the reciprocal lattice:

$$\epsilon_{\mathbf{k}} = \epsilon_{\mathbf{k}+\mathbf{G}} \ .$$
 (2)

Here ϵ_{k+G} is understood to refer to the same energy band as ϵ_k .

The result of this construction is known as the <u>periodic zone scheme</u>. The periodic property of the energy also can be seen easily from the central equation (7.27).

$$\psi = \sum_{k} C(k) e^{ikx} ,$$

$$(\lambda_k - \epsilon)C(k) + \sum_G U_G C(k - G) = 0 .$$

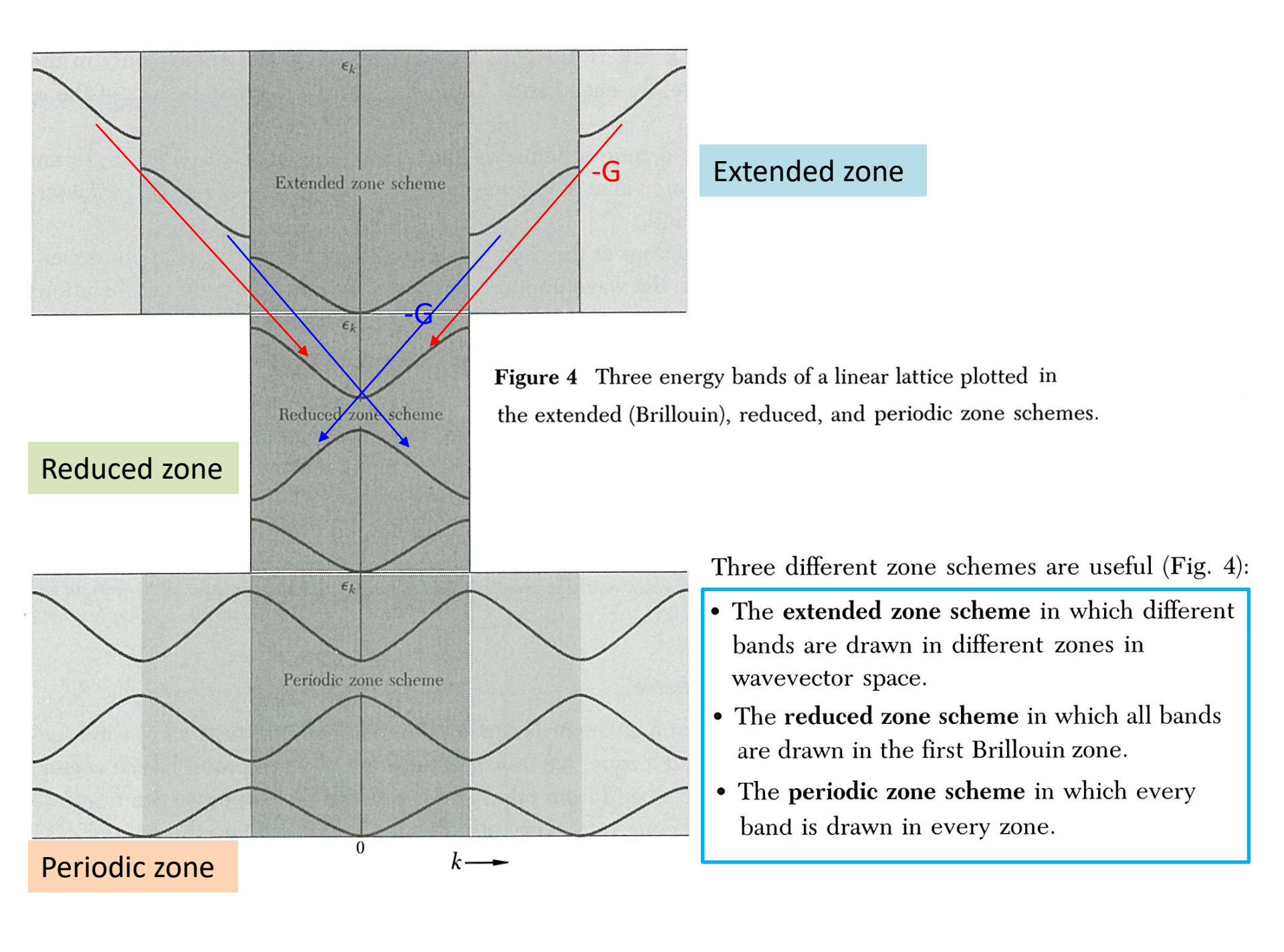
Consider for example an energy band of a simple cubic lattice as calculated in the tight-binding approximation in (13) below:

$$\epsilon_k = -\alpha - 2\gamma \left(\cos k_x a + \cos k_y a + \cos k_z a\right) , \qquad (3)$$

where α and γ are constants. A reciprocal lattice vector of the sc lattice is $\mathbf{G} = (2\pi/a)\hat{\mathbf{x}}$; if we add this vector to \mathbf{k} the only change in (3) is

$$\cos k_x a \to \cos (k_x + 2\pi/a)a = \cos (k_x a + 2\pi) ,$$

but this is identically equal to $\cos k_x a$. The energy is unchanged when the wavevector is increased by a reciprocal lattice vector, so that the energy is a periodic function of the wavevector.



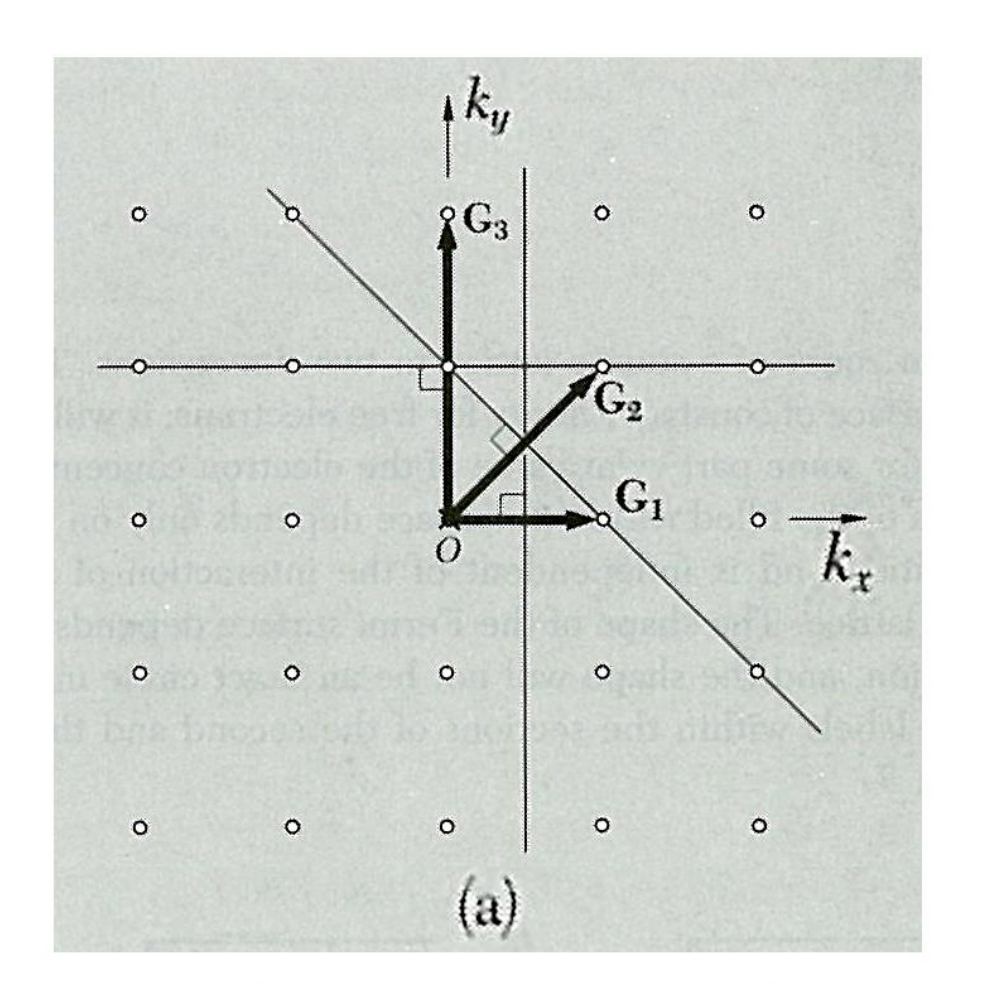
CONSTRUCTION OF FERMI SURFACES

We consider in Fig. 5 the analysis for a square lattice. The equation of the zone boundaries is $2\mathbf{k} \cdot \mathbf{G} + G^2 = 0$ and is satisfied if \mathbf{k} terminates on the plane normal to \mathbf{G} at the midpoint of \mathbf{G} . The first Brillouin zone of the square lattice is the area enclosed by the perpendicular bisectors of \mathbf{G}_1 and of the three reciprocal lattice vectors equivalent by symmetry to \mathbf{G}_1 in Fig. 5a. These four reciprocal lattice vectors are $\pm (2\pi/a)\hat{\mathbf{k}}_x$ and $\pm (2\pi/a)\hat{\mathbf{k}}_y$.

The second zone is constructed from G_2 and the three vectors equivalent to it by symmetry, and similarly for the third zone. The pieces of the second and third zones are drawn in Fig. 5b.

To determine the boundaries of some zones we have to consider sets of several nonequivalent reciprocal lattice vectors. Thus the boundaries of section 3_a of the third zone are formed from the perpendicular bisectors of three **G**'s, namely $(2\pi/a)\hat{\mathbf{k}}_x$; $(4\pi/a)\hat{\mathbf{k}}_y$; and $(2\pi/a)(\hat{\mathbf{k}}_x + \hat{\mathbf{k}}_y)$.

in Fig. 6



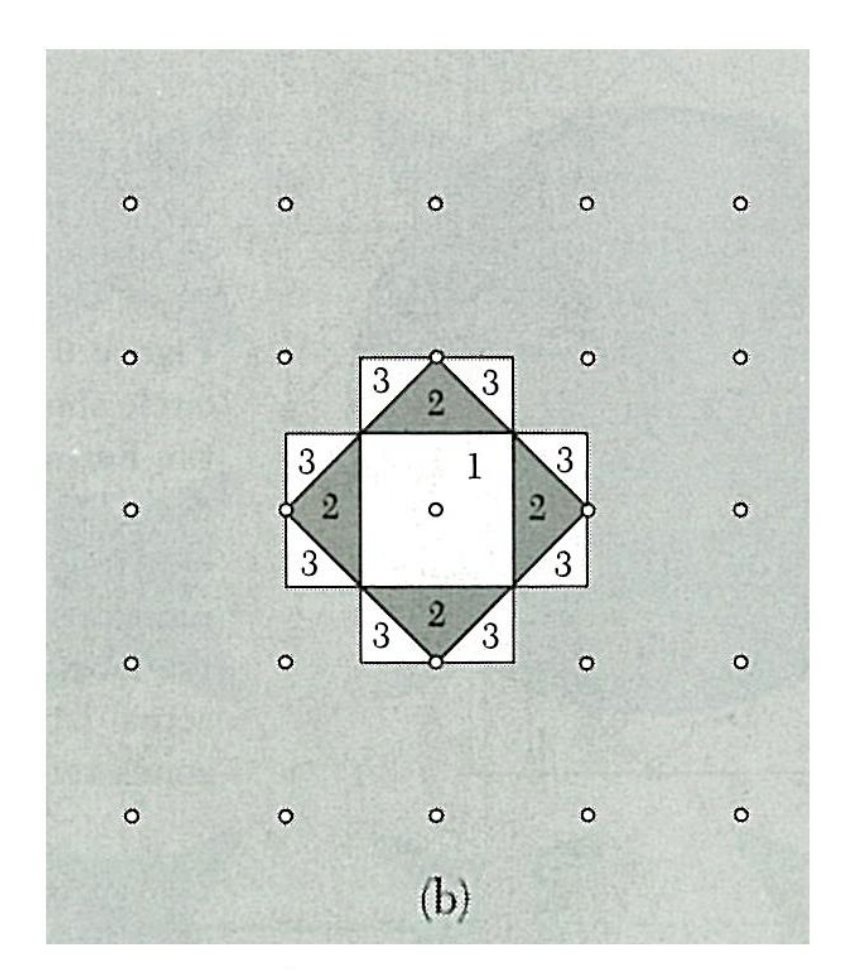


Figure 5 (a) Construction in k space of the first three Brillouin zones of a square lattice. The three shortest forms of the reciprocal lattice vectors are indicated as G_1 , G_2 , and G_3 . The lines drawn are the perpendicular bisectors of these G's. (b) On constructing all lines equivalent by symmetry to the three lines in (a) we obtain the regions in k space which form the first three Brillouin zones. The numbers denote the zone to which the regions belong; the numbers here are ordered according to the length of the vector G involved in the construction of the outer boundary of the region.

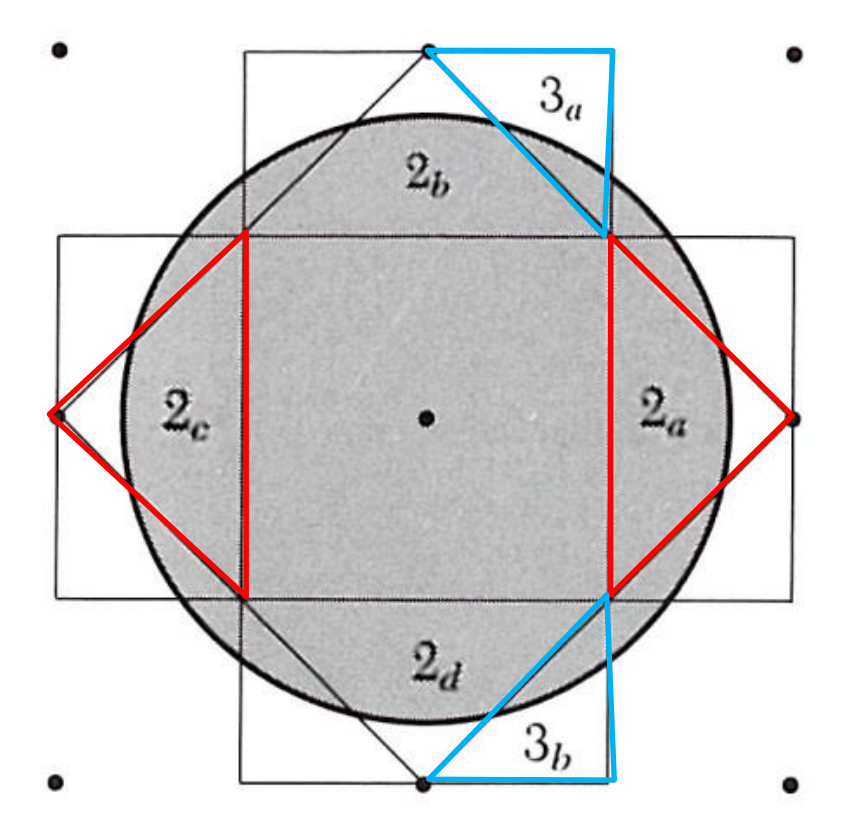


Figure 6 Brillouin zones of a square lattice in two dimensions. The circle shown is a surface of constant energy for free electrons; it will be the Fermi surface for some particular value of the electron concentration. The total area of the filled region in **k** space depends only on the electron concentration and is independent of the interaction of the electrons with the lattice. The shape of the Fermi surface depends on the lattice interaction, and the shape will not be an exact circle in an actual lattice. The labels within the sections of the second and third zones refer to Fig. 7.

The free electron Fermi surface for an arbitrary electron concentration is shown in Fig. 6. It is inconvenient to have sections of the Fermi surface that belong to the same zone appear detached from one another. The detachment can be repaired by a transformation to the reduced zone scheme.

We take the triangle labeled 2_a and move it by a reciprocal lattice vector $\mathbf{G} = -(2\pi/a)\hat{\mathbf{k}}_x$ such that the triangle reappears in the area of the first Brillouin zone (Fig. 7). Other reciprocal lattice vectors will shift the triangles 2_b , 2_c , 2_d to other parts of the first zone, completing the mapping of the second zone into the reduced zone scheme. The parts of the Fermi surface falling in the second zone are now connected, as shown in Fig. 8.

A third zone is assembled into a square in Fig. 8, but the parts of the Fermi surface still appear disconnected. When we look at it in the periodic zone scheme (Fig. 9), the Fermi surface forms a lattice of rosettes.

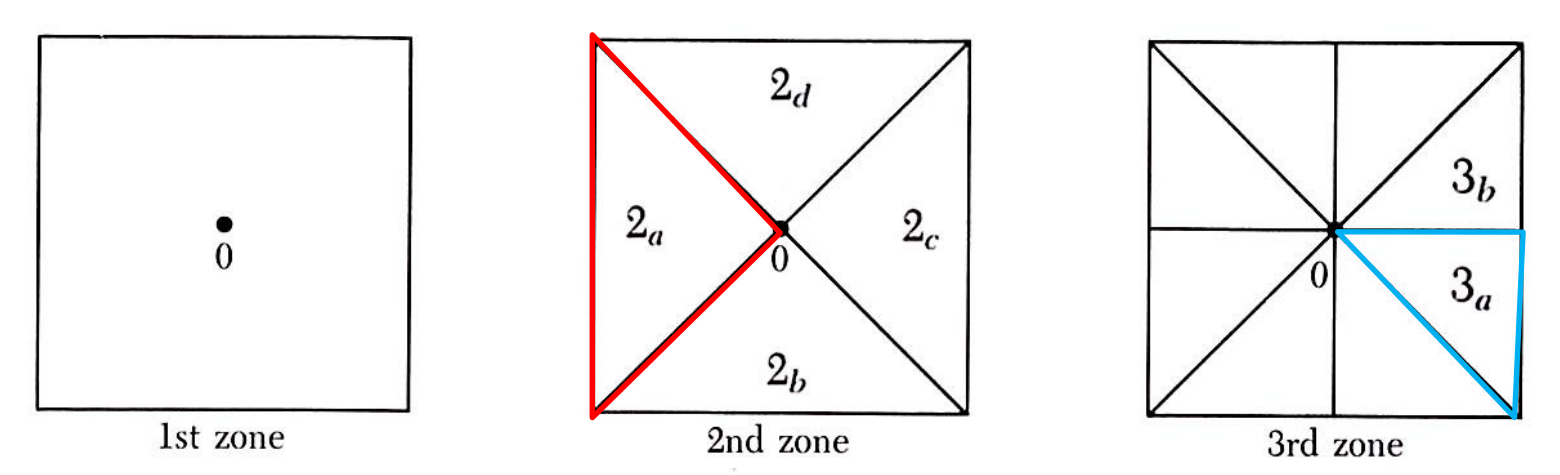


Figure 7 Mapping of the first, second, and third Brillouin zones in the reduced zone scheme. The sections of the second zone in Fig. 6 are put together into a square by translation through an appropriate reciprocal lattice vector. A different G is needed for each piece of a zone.

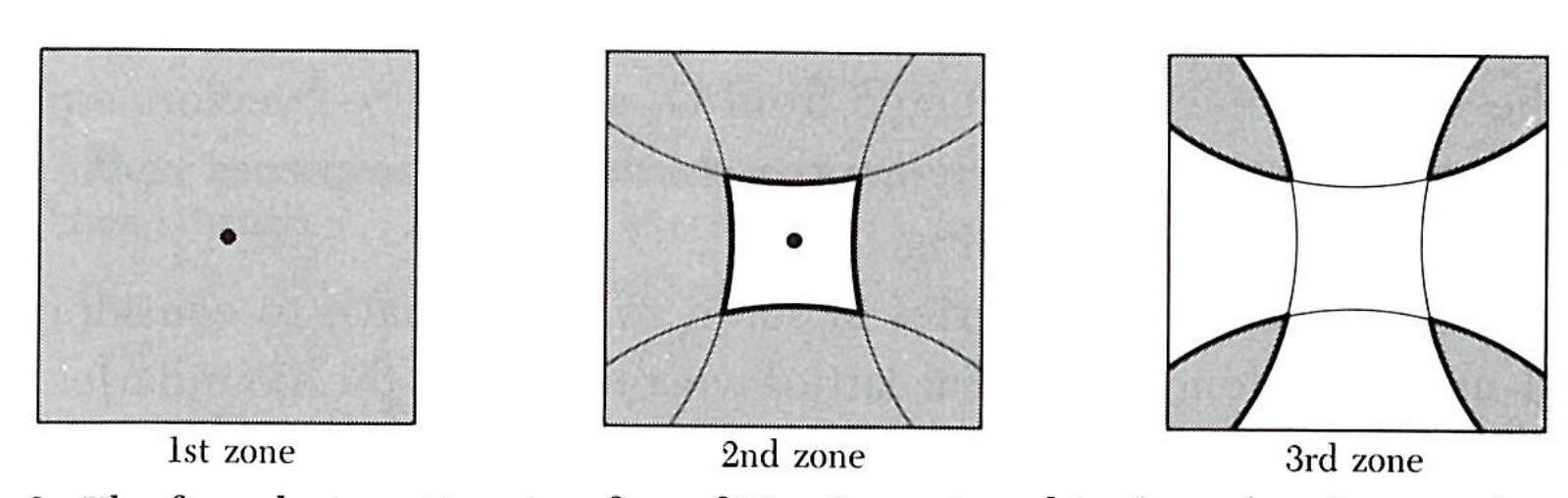
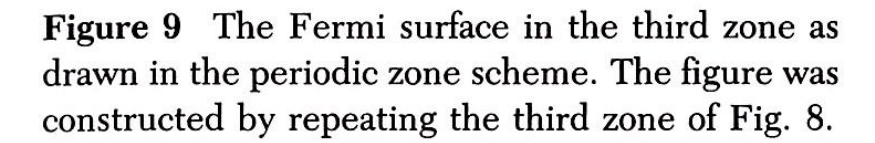
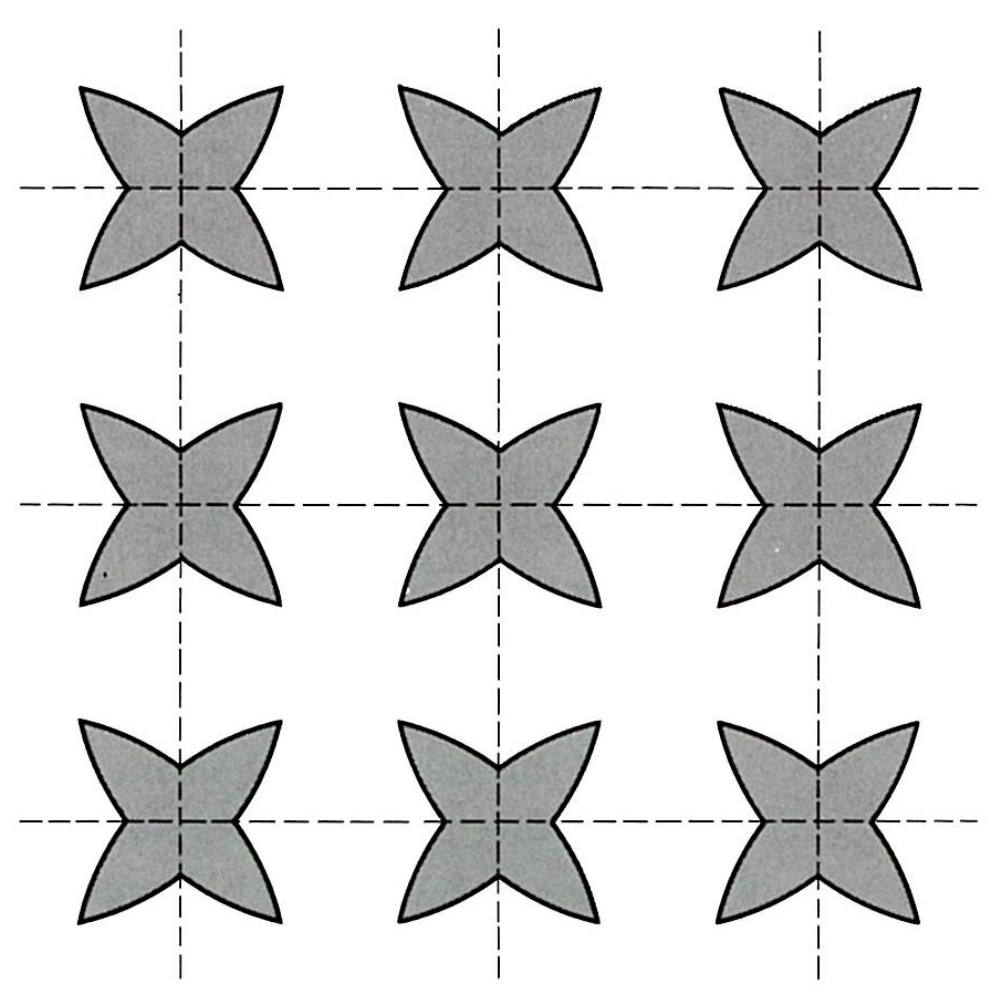


Figure 8 The free electron Fermi surface of Fig. 6, as viewed in the reduced zone scheme. The shaded areas represent occupied electron states. Parts of the Fermi surface fall in the second, third, and fourth zones. The fourth zone is not shown. The first zone is entirely occupied.

Periodic zone scheme





Nearly Free Electrons

How do we go from Fermi surfaces for free electrons to Fermi surfaces for nearly free electrons? We can make approximate constructions freehand by the use of four facts:

- The interaction of the electron with the periodic potential of the crystal causes energy gaps at the zone boundaries.
- Almost always the Fermi surface will intersect zone boundaries perpendicularly (see below).

 See page 37, 38, 39
- The crystal potential will round out sharp corners in the Fermi surfaces.
- The total volume enclosed by the Fermi surface depends only on the electron concentration and is independent of the details of the lattice interaction.

We cannot make quantitative statements without calculation, but qualitatively we expect the Fermi surfaces in the second and third zones of Fig. 8 to be changed as shown in Fig. 10.

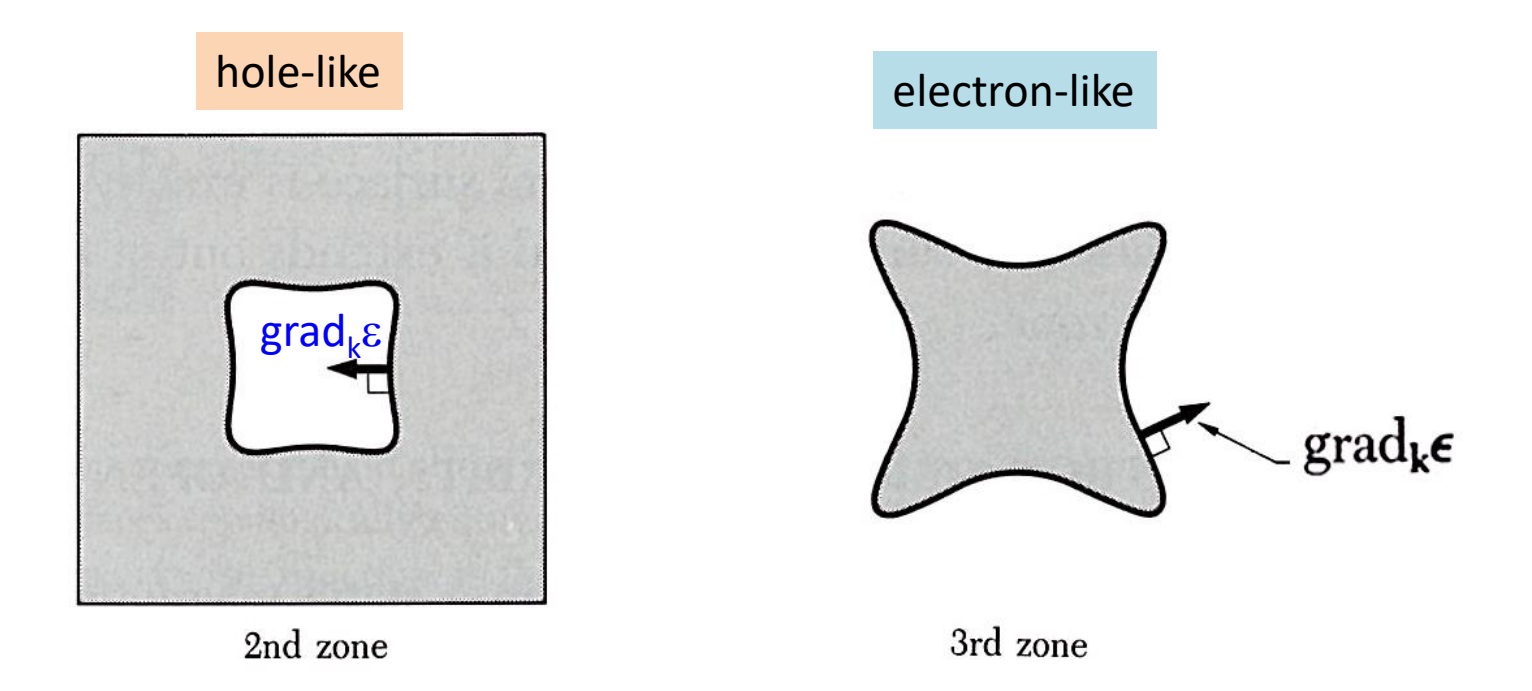


Figure 10 Qualitative impression of the effect of a weak periodic crystal potential on the Fermi surface of Fig. 8. At one point on each Fermi surface we have shown the vector $\operatorname{grad}_{\mathbf{k}}\boldsymbol{\epsilon}$. In the second zone the energy increases toward the interior of the figure, and in the third zone the energy increases toward the exterior. The shaded regions are filled with electrons and are lower in energy than the unshaded regions. We shall see that a Fermi surface like that of the third zone is electron-like, whereas one like that of the second zone is holelike. It is said that electrons sink and holes float.

Freehand impressions of the Fermi surfaces derived from free electron surfaces are useful. Fermi surfaces for free electrons are constructed by a procedure credited to Harrison, Fig. 11. The reciprocal lattice points are determined, and a free-electron sphere of radius appropriate to the electron concentration is drawn around each point. Any point in k space that lies within at least one sphere corresponds to an occupied state in the first zone. Points within at least two spheres correspond to occupied states in the second zone, and similarly for points in three or more spheres.

We said earlier that the alkali metals are the simplest metals, with weak interactions between the conduction electrons and the lattice. Because the alkalis have only one valence electron per atom, the first Brillouin zone boundaries are distant from the approximately spherical Fermi surface that fills one-half of the volume of the zone. It is known by calculation and experiment that the Fermi surface of Na is closely spherical, and that for Cs the Fermi surface is deformed by perhaps 10 percent from a sphere.

The divalent metals Be and Mg also have weak lattice interactions and nearly spherical Fermi surfaces. But because they have two valence electrons each, the Fermi surface encloses twice the volume in **k** space as for the alkalis. That is, the volume enclosed by the Fermi surface is exactly equal to that of a zone, but because the surface is spherical it extends out of the first zone and into the second zone.

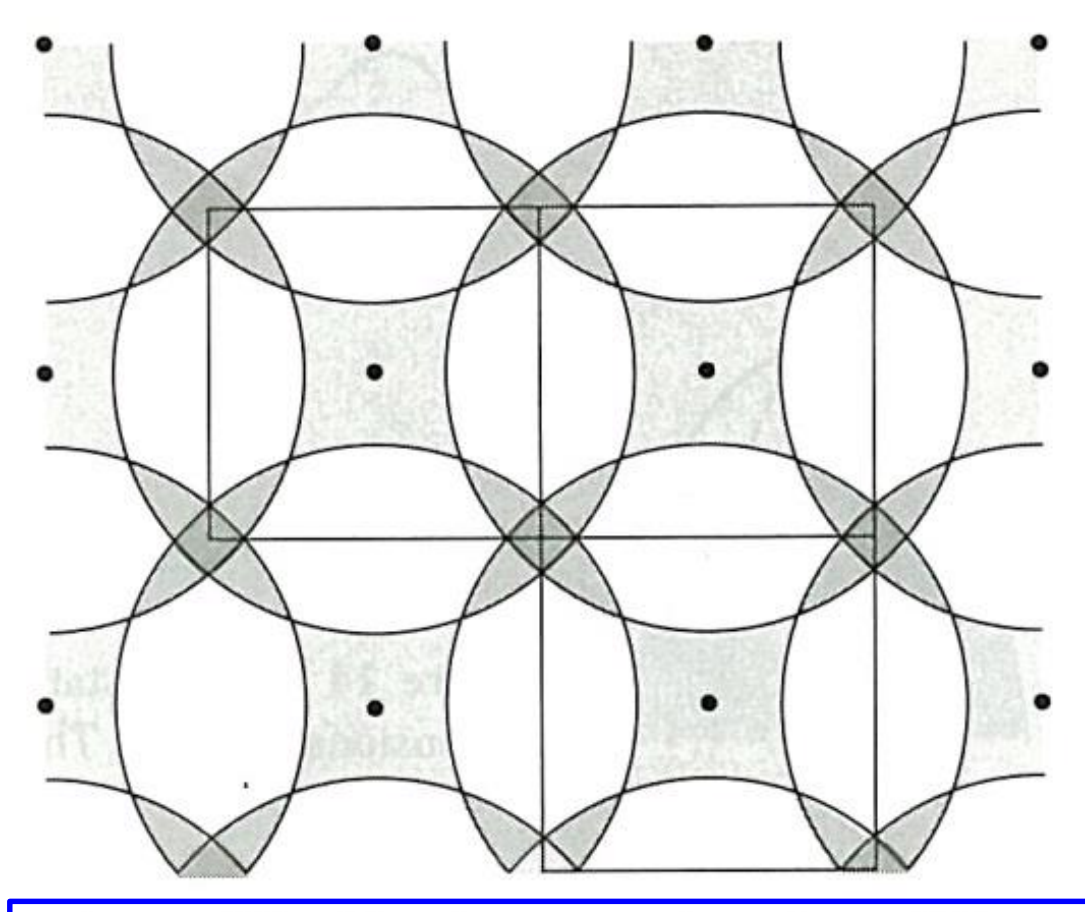


Figure 11 Harrison construction of free electron Fermi surfaces on the second, third, and fourth zones for a square lattice. The Fermi surface encloses the entire first zone, which therefore is filled with electrons.

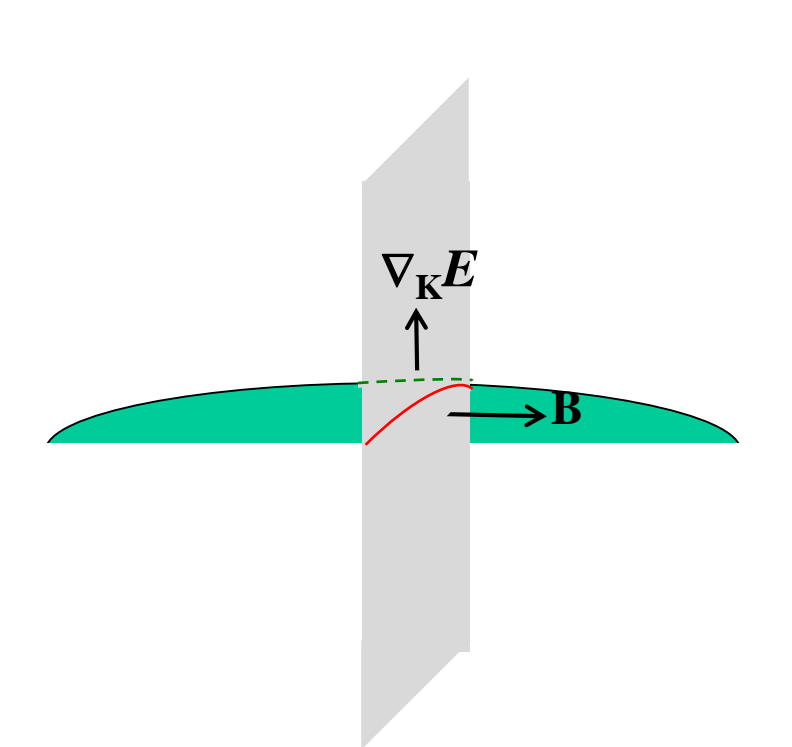
ELECTRON ORBITS, HOLE ORBITS, AND OPEN ORBITS

We saw in Eq. (8.7) that electrons in a static magnetic field move on a curve of constant energy on a plane normal to **B**. An electron on the Fermi surface will move in a curve on the Fermi surface, because this is a surface of constant energy. Three types of orbits in a magnetic field are shown in Fig. 12.

The closed orbits of (a) and (b) are traversed in opposite senses. Because particles of opposite charge circulate in a magnetic field in opposite senses, we say that one orbit is electronlike and the other orbit is holelike. Electrons in holelike orbits move in a magnetic field as if endowed with a positive charge. This is consistent with the treatment of holes in Chapter 8.

In (c) the orbit is not closed: the particle on reaching the zone boundary at A is instantly umklapped back to B, where B is equivalent to B' because they are connected by a reciprocal lattice vector. Such an orbit is called an open orbit. Open orbits have an important effect on the magnetoresistance.

Vacant orbitals near the top of an otherwise filled band give rise to holelike orbits, as in Figs. 13 and 14. A view of a possible energy surface in three dimensions is given in Fig. 15.



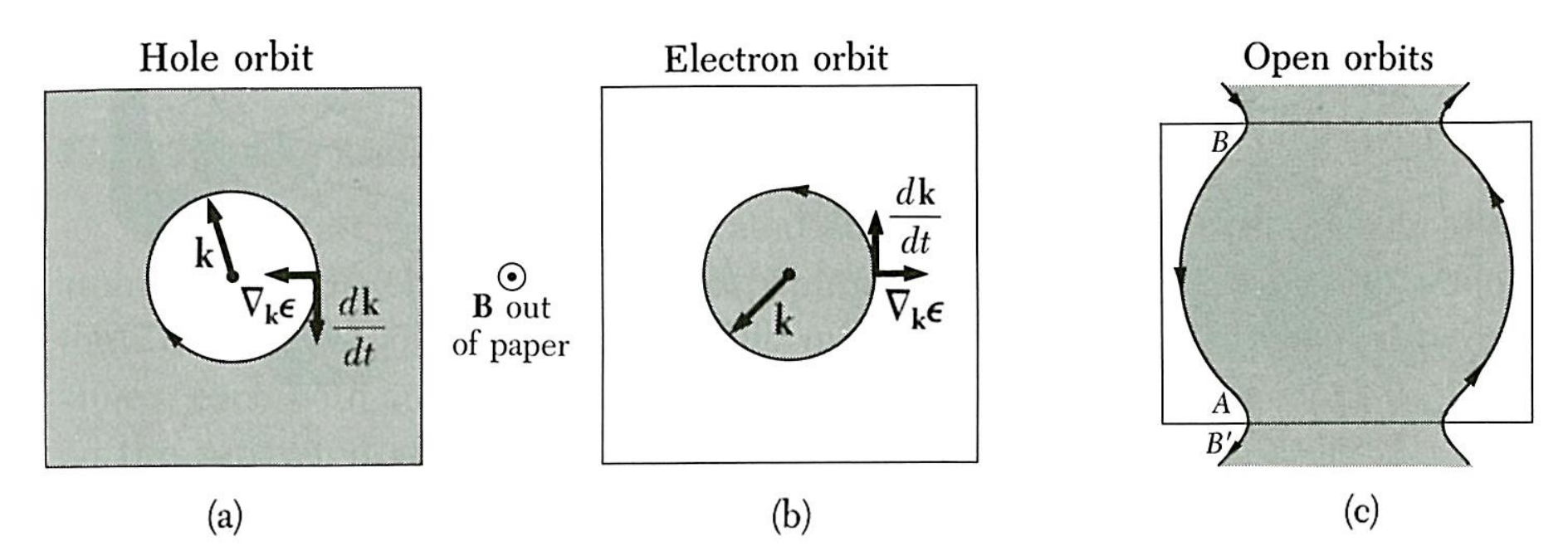
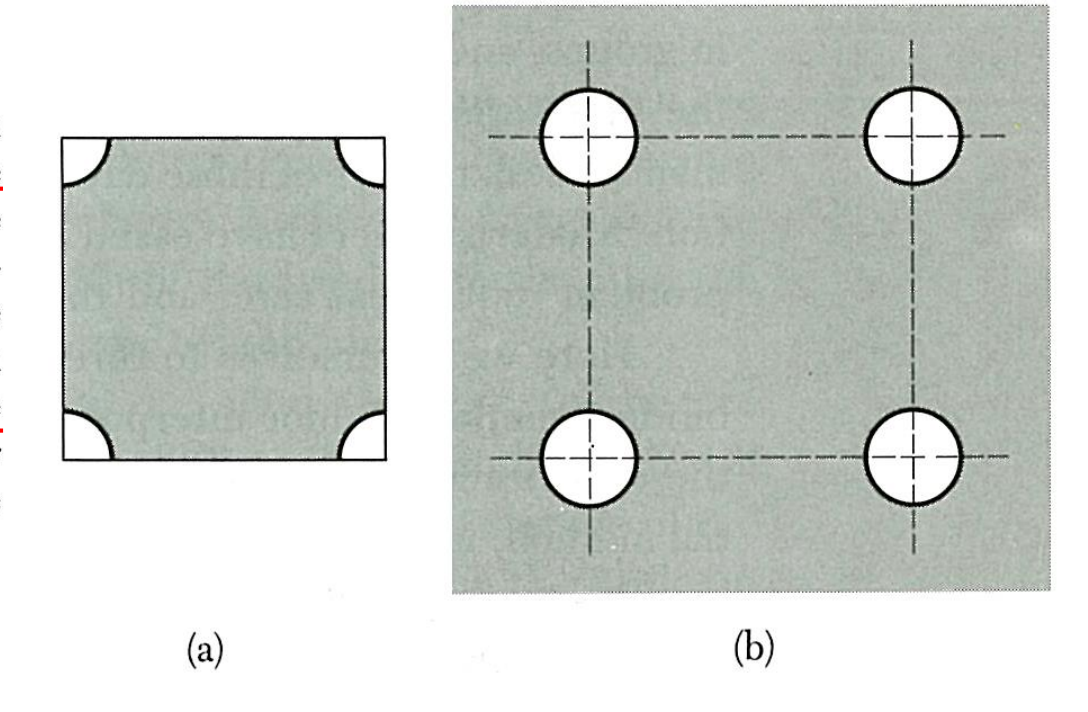


Figure 12 Motion in a magnetic field of the wavevector of an electron on the Fermi surface, in (a) and (b) for Fermi surfaces topologically equivalent to those of Fig. 10. In (a) the wavevector moves around the orbit in a clockwise direction; in (b) the wavevector moves around the orbit in a counterclockwise direction. The direction in (b) is what we expect for a free electron of charge -e: the smaller k values have the lower energy, so that the filled electron states lie inside the Fermi surface. We call the orbit in (b) electronlike. The sense of the motion in a magnetic field is opposite in (a) to that in (b), so that we refer to the orbit in (a) as holelike. A hole moves as a particle of positive charge e. In (c) for a rectangular zone we show the motion on an open orbit in the periodic zone scheme. This is topologically intermediate between a hole orbit and an electron orbit.

Orbits that enclose filled states are <u>electron orbits</u>. Orbits that enclose empty states are <u>hole orbits</u>. Orbits that move from zone to zone without closing are <u>open orbits</u>.

Figure 13 (a) Vacant states at the corners of an almost-filled band, drawn in the reduced zone scheme. (b) In the periodic zone scheme the various parts of the Fermi surface are connected. Each circle forms a holelike orbit. The different circles are entirely equivalent to each other, and the density of states is that of a single circle. (The orbits need not be true circles: for the lattice shown it is only required that the orbits have fourfold symmetry.)



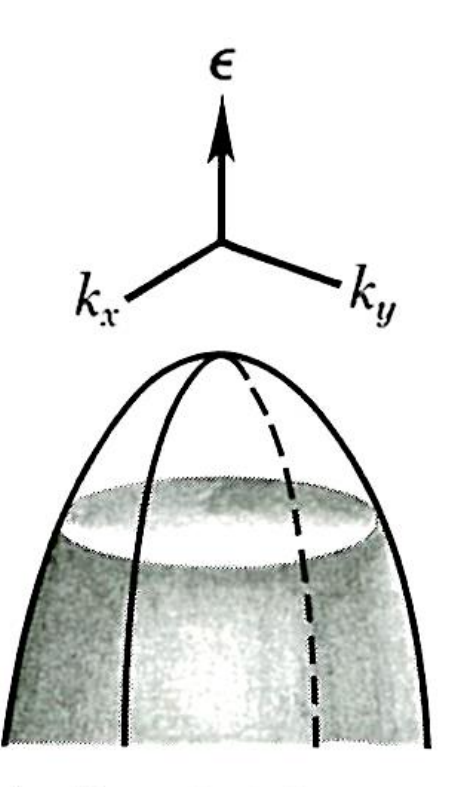


Figure 14 Vacant states near the top of an almost filled band in a two-dimensional crystal. This figure is equivalent to Fig. 12a.

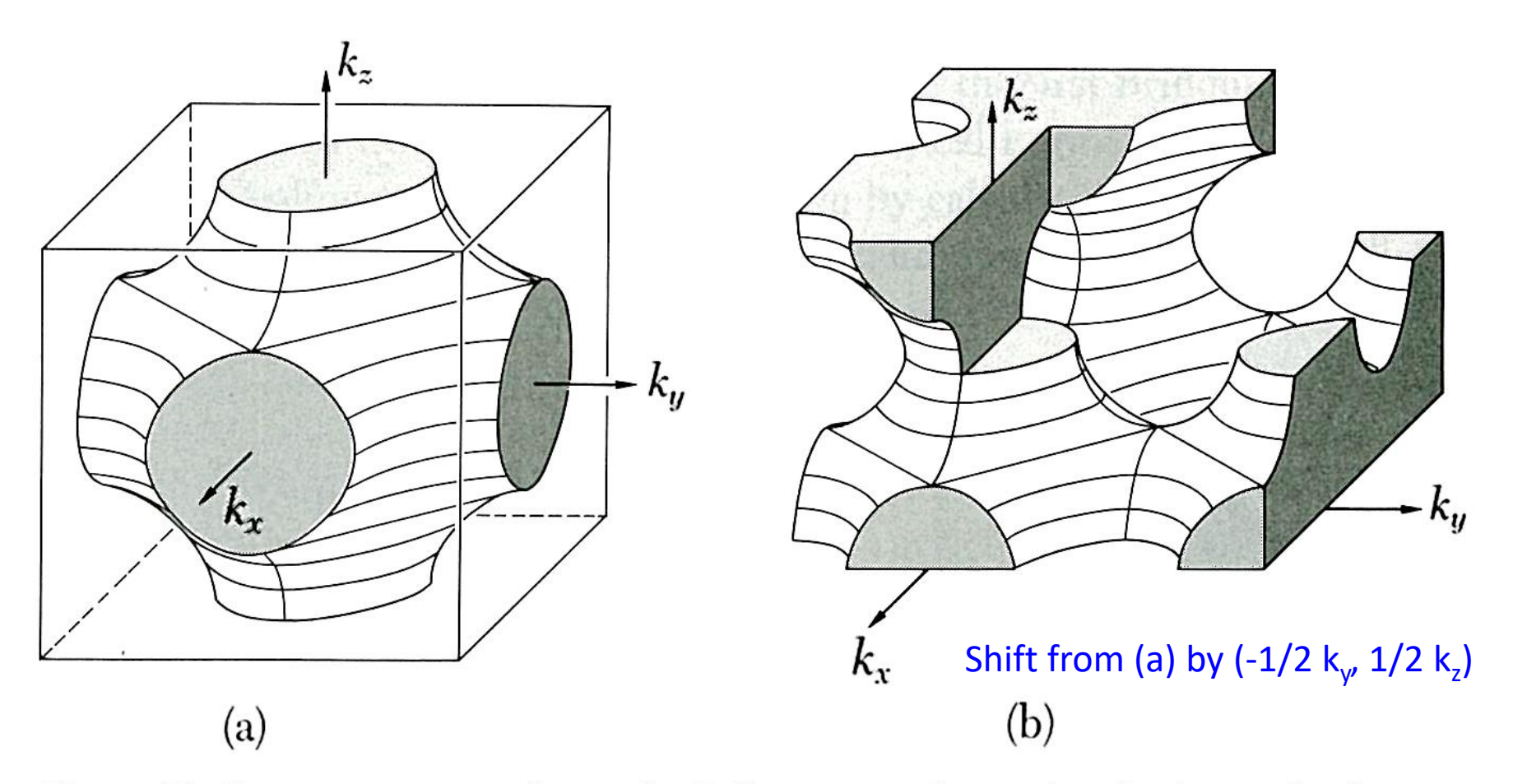


Figure 15 Constant energy surface in the Brillouin zone of a simple cubic lattice, for the assumed energy band $\epsilon_k = -\alpha - 2\gamma(\cos k_x a + \cos k_y a + \cos k_z a)$. (a) Constant energy surface $\epsilon = -\alpha$. The filled volume contains one electron per primitive cell. (b) The same surface exhibited in the periodic zone scheme. The connectivity of the orbits is clearly shown. Can you find electron, hole, and open orbits for motion in a magnetic field $B\hat{z}$? (A. Sommerfeld and H. A. Bethe.)

Ashcroft Mermin
Chapter 9
Electrons in a weak periodic potential

BRILLOUIN ZONES

Using the theory of electrons in a weak periodic potential to determine the complete band structure of a three-dimensional crystal leads to geometrical constructions of great complexity. It is often most important to determine the Fermi surface (page 141) and the behavior of the $\mathcal{E}_n(\mathbf{k})$ in its immediate vicinity.

In doing this for weak potentials, the procedure is first to draw the free electron Fermi sphere centered at $\mathbf{k} = \mathbf{0}$. Next, one notes that the sphere will be deformed in a manner of which Figure 9.6 is characteristic¹¹ when it crosses a Bragg plane and in a correspondingly more complex way when it passes near several Bragg planes. When the effects of all Bragg planes are inserted, this leads to a representation of the Fermi surface as a fractured sphere in the extended-zone scheme. To construct the portions of the Fermi surface lying in the various bands in the repeated-zone scheme one can make a similar construction, starting with free electron spheres centered about all reciprocal lattice points. To construct the Fermi surface in the reduced-zone scheme, one can translate all the pieces of the single fractured sphere back into the first zone through reciprocal lattice vectors. This procedure is made systematic through the geometrical notion of the higher Brillouin zones.

The Fermi surface always intersects Brillouin zone boundary perpendicularly

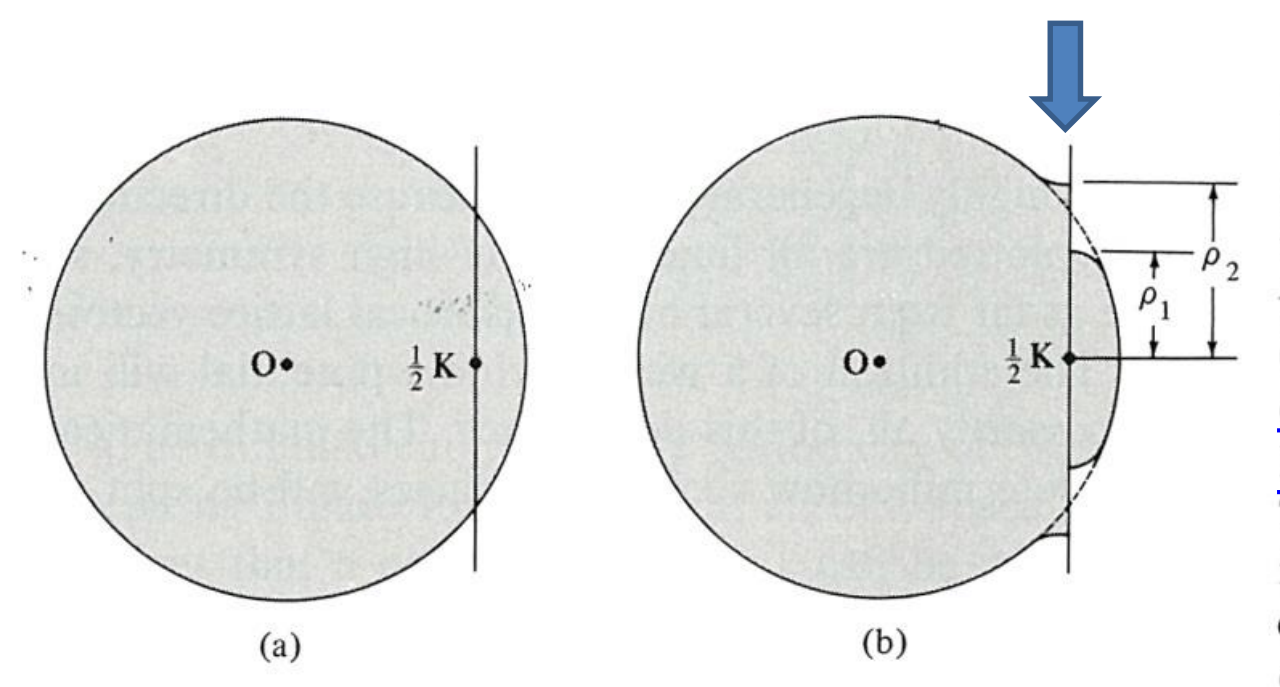


Figure 9.6

(a) Free electron sphere cutting Bragg plane located at $\frac{1}{2}$ K from the origin ($U_K = 0$). (b) Deformation of the free electron sphere near the Bragg plane when $U_K \neq 0$. The constant-energy surface intersects the plane in two circles, whose radii are calculated in Problem 1.

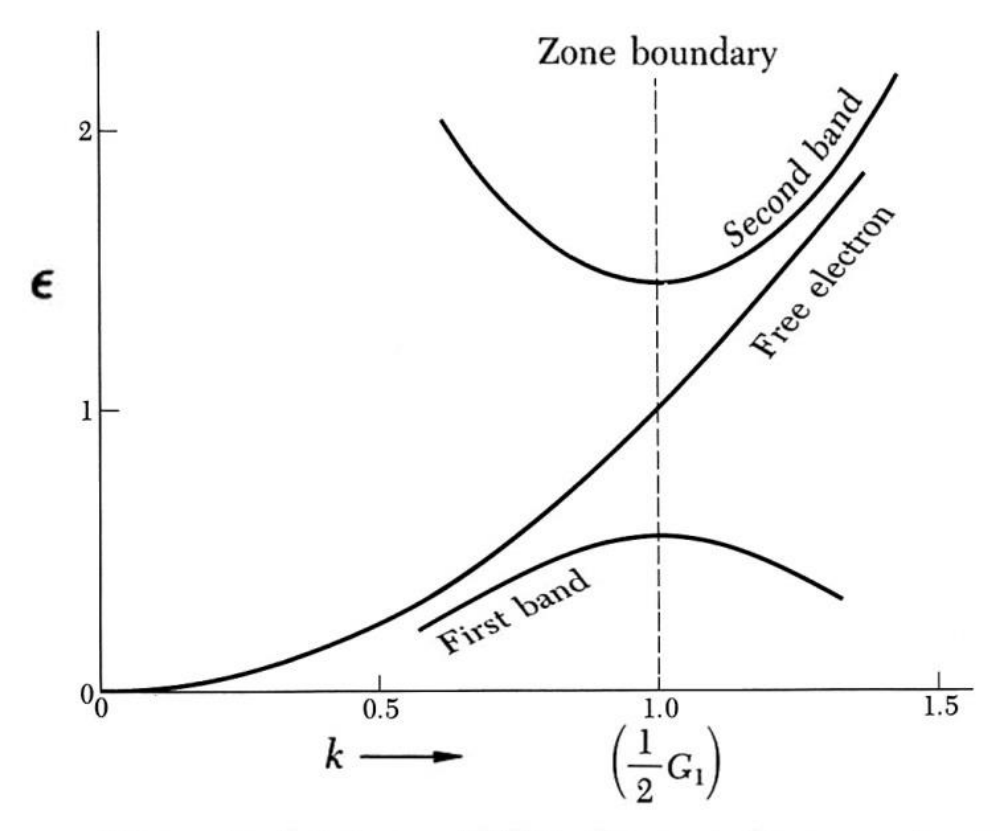


Figure 9 Solutions of (50) in the periodic zone scheme, in the region near a boundary of the first Brillouin zone. The units are such that U=-0.45; G=2, and $\hbar^2/m=1$. The free electron curve is drawn for comparison. The energy gap at the zone boundary is 0.90. The value of U has deliberately been chosen large for this illustration, too large for the two-term approximation to be accurate.

Recall that the first Brillouin zone is the Wigner-Seitz primitive cell of the reciprocal lattice (pages 73 and 89), i.e. the set of points lying closer to $\mathbf{K} = \mathbf{0}$ than to any other reciprocal lattice point. Since Bragg planes bisect the lines joining the origin to points of the reciprocal lattice, one can equally well define the first zone as the set of points that can be reached from the origin without crossing any Bragg planes.¹²

Higher Brillouin zones are simply other regions bounded by the Bragg planes, defined as follows:

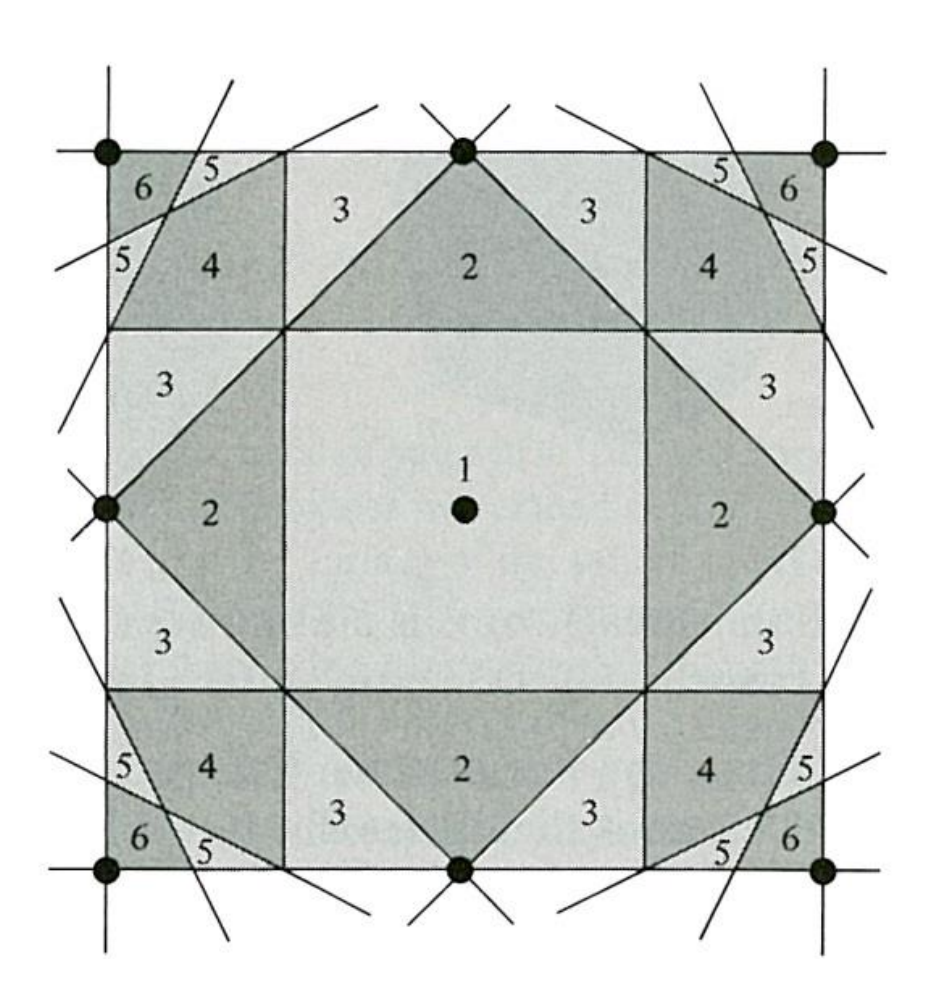
The first Brillouin zone is the set of points in k-space that can be reached from the origin without crossing any Bragg plane. The second Brillouin zone is the set of points that can be reached from the first zone by crossing only one Bragg plane. The (n+1)th Brillouin zone is the set of points not in the (n-1)th zone that can be reached from the nth zone by crossing only one Bragg plane.

Alternatively, the *nth Brillouin zone* can be defined as the set of points that can be reached from the origin by crossing n-1 Bragg planes, but no fewer.

These definitions are illustrated in two dimensions in Figure 9.7. The surface of the first three zones for the fcc and bcc lattices are shown in Figure 9.8. Both definitions emphasize the physically important fact that the zones are bounded by Bragg planes. Thus they are regions at whose surfaces the effects of a weak periodic potential are important (i.e., first order), but in whose interior the free electron energy levels are only perturbed in second order.

Figure 9.7

Illustration of the definition of the Brillouin zones for a two-dimensional square Bravais lattice. The reciprocal lattice is also a square lattice of side b. The figure shows all Bragg planes (lines, in two dimensions) that lie within the square of side 2b centered on the origin. These Bragg planes divide that square into regions belonging to zones 1 to 6. (Only zones 1, 2, and 3 are entirely contained within the square, however.)



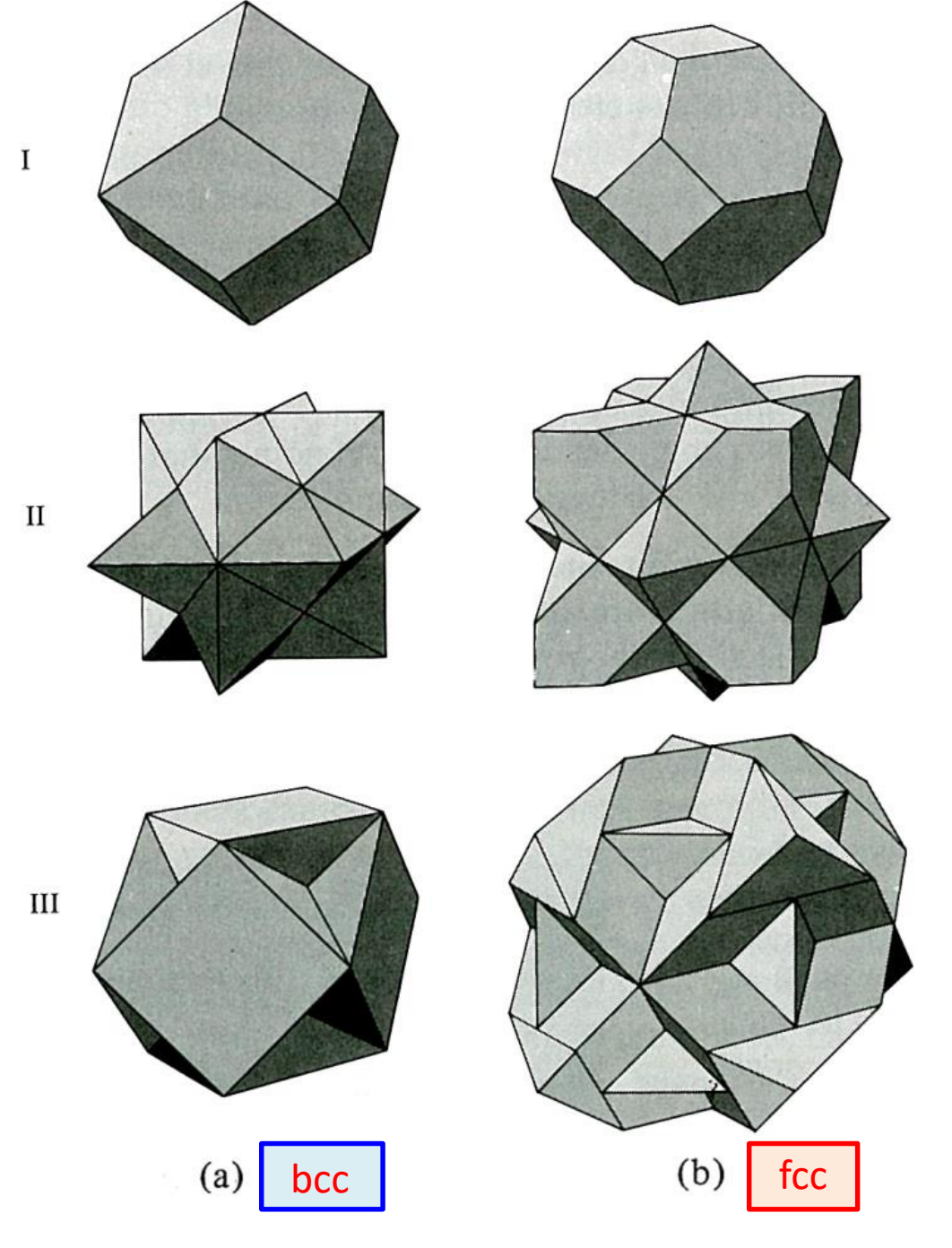


Figure 9.8

Surfaces of the first, second. and third Brillouin zones for (a) body-centered cubic and (b) face-centered cubic crystals. (Only the exterior surfaces are shown. It follows from the definition on page 163 that the interior surface of the nth zone is identical to the exterior surface of the (n-1)th. zone.) Evidently the surfaces bounding the zones become increasingly complex as the zone number increases. In practice it is often simplest to construct free electron Fermi surfaces by procedures (such as those described in Problem 4) that avoid making use of the explicit form of the Brillouin zones. (After R. Lück, doctoral dissertation, Technische Hochschule, Stuttgart, 1965.)

It is very important to note that each Brillouin zone is a primitive cell of the reciprocal lattice. This is because the nth Brillouin zone is simply the set of points that have the origin as the nth nearest reciprocal lattice point (a reciprocal lattice point **K** is nearer to a point **k** than **k** is to the origin if and only if **k** is separated from the origin by the Bragg plane determined by **K**). Given this, the proof that the nth Brillouin zone is a primitive cell is identical to the proof on page 73 that the Wigner-Seitz cell (i.e., the first Brillouin zone) is primitive, provided that the phrase "nth nearest neighbor" is substituted for "nearest neighbor" throughout the argument.

Because each zone is a primitive cell, there is a simple algorithm for constructing the branches of the Fermi surface in the repeated-zone scheme¹³:

- 1. Draw the free electron Fermi sphere.
- 2. Deform it slightly (as illustrated in Figure 9.6) in the immediate vicinity of every Bragg plane. (In the limit of exceedingly weak potentials this step is sometimes ignored to a first approximation.)
- 3. Take that portion of the surface of the free electron sphere lying within the *n*th Brillouin zone, and translate it through all reciprocal lattice vectors. The resulting surface is the branch of the Fermi surface (conventionally assigned to the *n*th band) in the repeated-zone scheme.¹⁴

Generally speaking, the effect of the weak periodic potential on the surfaces constructed from the free electron Fermi sphere without step 2, is simply to round off the sharp edges and corners. If, however, a branch of the Fermi surface consists of very small pieces of surface (surrounding either occupied or unoccupied levels, known as "pockets of electrons" or "pockets of holes"), then a weak periodic potential may cause these to disappear. In addition, if the free electron Fermi surface has parts with a very narrow cross section, a weak periodic potential may cause it to become disconnected at such points.

Some further constructions appropriate to the discussion of almost free electrons in fcc crystals are illustrated in Figure 9.10. These free-electron-like Fermi surfaces are of great importance in understanding the real Fermi surfaces of many metals. This will be illustrated in Chapter 15.

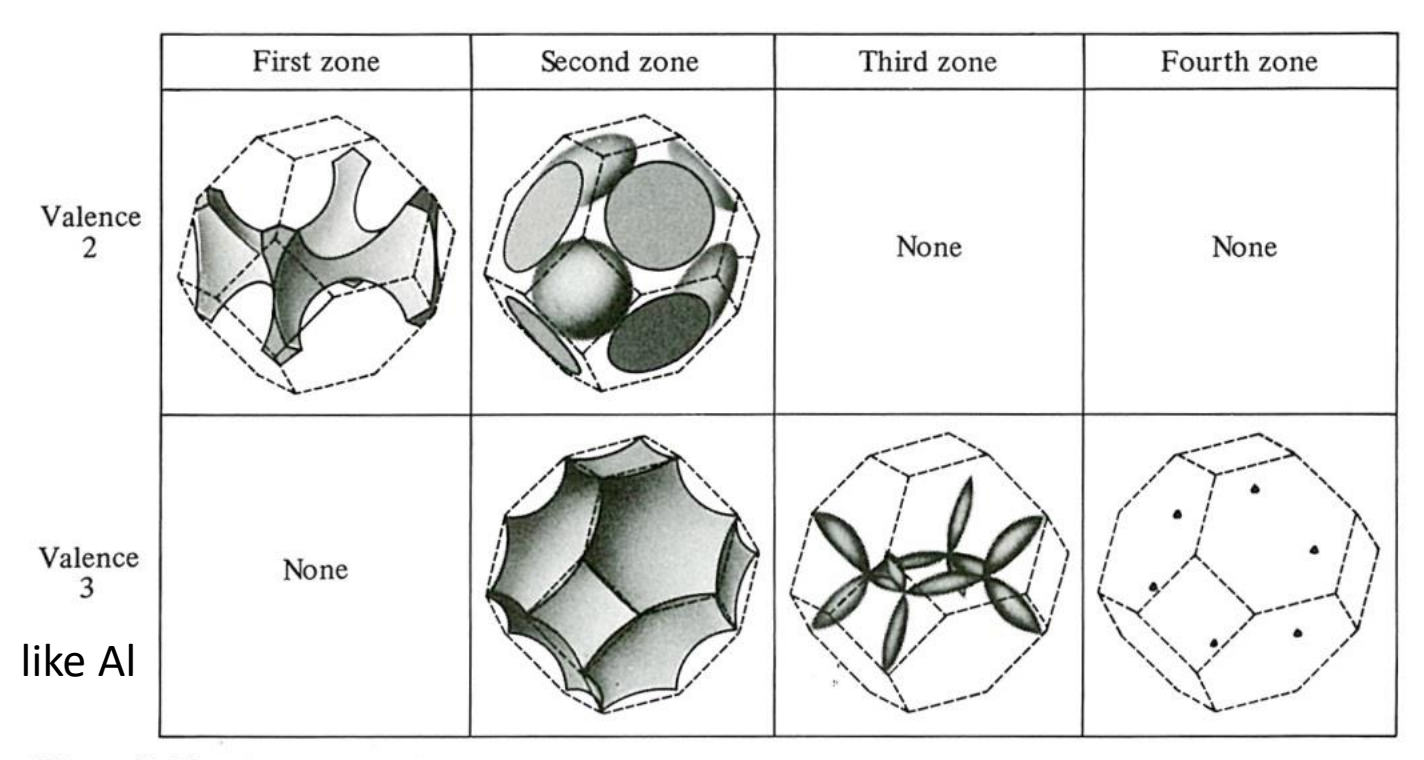


Figure 9.10

The free electron Fermi surfaces for face-centered cubic metals of valence 2 and 3. (For valence 1 the surface lies entirely within the interior of the first zone and therefore remains a sphere to lowest order; the surface for valence 4 is shown in Figure 9.9.) All branches of the Fermi surface are shown. The primitive cells in which they are displayed have the shape and orientation of the first Brillouin zone. However, the cell is actually the first zone (i.e., is centered on $\mathbf{K} = \mathbf{0}$) only in the figures illustrating the second zone surfaces. In the first and third zone figures $\mathbf{K} = \mathbf{0}$ lies at the center of one of the horizontal faces, while for the fourth zone figure it lies at the center of the hexagonal face on the upper right (or the parallel face opposite it (hidden)). The six tiny pockets of electrons constituting the fourth zone surface for valence 3 lie at the corners of the regular hexagon given by displacing that hexagonal face in the [111] direction by half the distance to the face opposite it. (After W. Harrison, *Phys. Rev.* 118, 1190 (1960).) Corresponding constructions for body-centered cubic metals can be found in the Harrison paper.

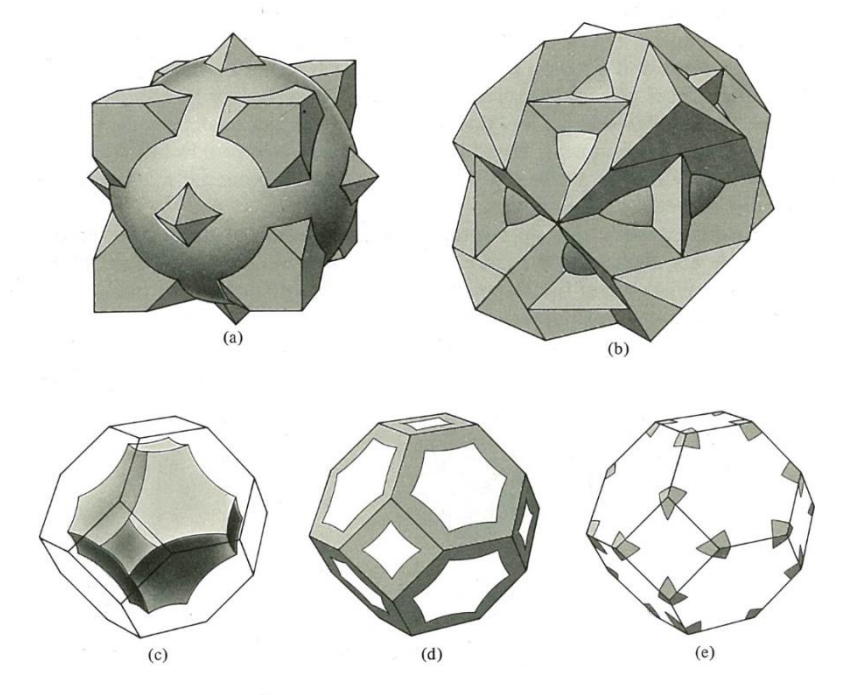


Figure 9.9

The free electron Fermi sphere for a face-centered cubic metal of valence 4. The first zone lies entirely within the interior of the sphere, and the sphere does not extend beyond the fourth zone. Thus the only zone surfaces intersected by the surface of the sphere are the (exterior) surfaces of the second and third zones (cf. Figure 9.8b). The second-zone Fermi surface consists of those parts of the surface of the sphere lying entirely within the polyhedron bounding the second zone (i.e., all of the sphere except the parts extending beyond the polyhedron in (a)). When translated through reciprocal lattice vectors into the first zone, the pieces of the second-zone surface give the simply connected figure shown in (c). (It is known as a "hole surface"; the levels it encloses have higher energies than those outside). The third-zone Fermi surface consists of those parts of the surface of the sphere lying outside of the second zone (i.e., the parts extending beyond the polyhedron in (a)) that do not lie outside the third zone (i.e., that are contained within the polyhedron shown in (b)). When translated through reciprocal lattice vectors into the first zone, these pieces of sphere give the multiply connected structure shown in (d). The fourth-zone Fermi surface consists of the remaining parts of the surface of the sphere that lie outside the third zone (as shown in (b)). When translated through reciprocal lattice vectors into the first zone they form the "pockets of electrons" shown in (e). For clarity (d) and (e) show only the intersection of the third and fourth zone Fermi surfaces with the surface of the first zone. (From R. Lück, op. cit.)